

X-RISK-CC pilot areas (top) and the pilot area of Gorenjska – Sora catchment (bottom)

# DROUGHT AND HEATWAVES IN GORENJSKA – SORA CATCHMENT

Slovenia

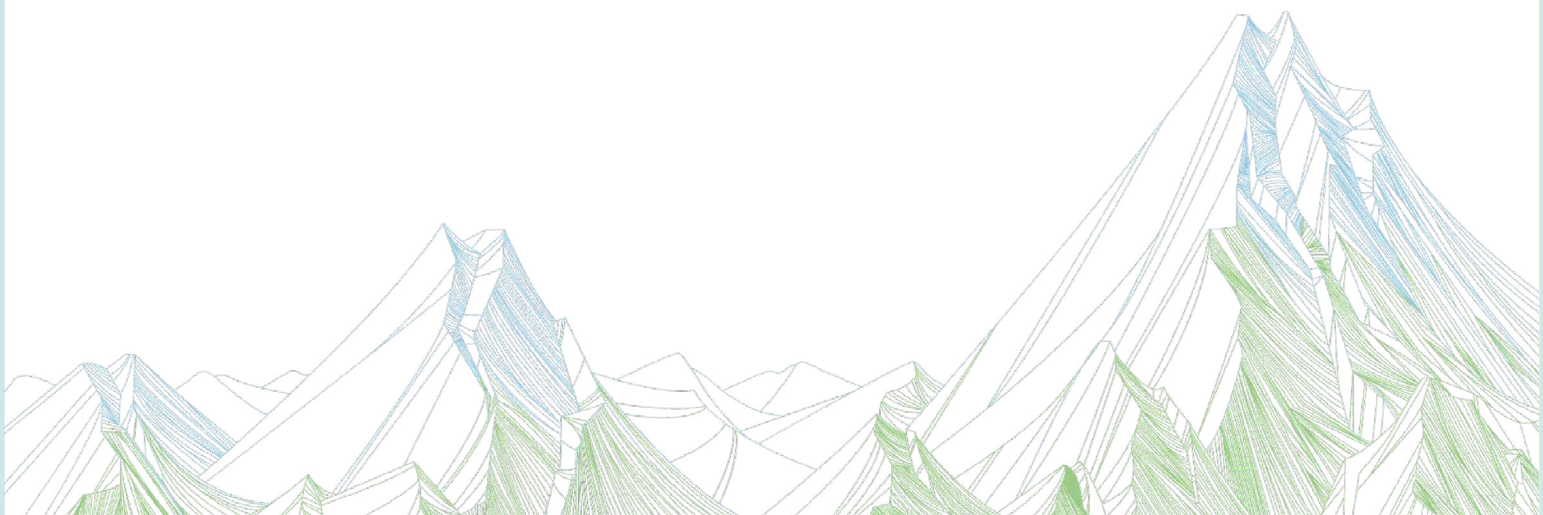


Pilot report prepared by Slovenian Environment Agency, GeoSphere Austria and EURAC Research with the support of the X-RISK-CC partnership

# TABLE OF CONTENTS



<b>KEY MESSAGES</b>	<b>3</b>
<b>PAST EXTREME EVENTS IN FOCUS</b>	<b>4</b>
<b>DEFINITION OF METEOROLOGICAL AND GROUNDWATER EXTREMES</b>	<b>5</b>
<b>TYPICAL SYNOPTIC SITUATION LEADING TO THE EXTREME EVENT</b>	<b>9</b>
<b>CHARACTERISTICS OF EXTREME EVENTS IN THE PAST</b>	<b>11</b>
<b>WHAT TO EXPECT IN THE FUTURE?</b>	<b>20</b>
<b>METHODOLOGY</b>	<b>24</b>



# KEY MESSAGES



## COMPOUND DROUGHT AND HEATWAVE EVENTS

- In the last two decades, several severe or extreme droughts have been recorded in Sora catchment, with the most severe observed in the 2003 growing season, the summer 2013 and the 2022 growing season, while moderately dry conditions have occurred more frequently. The most recent drought in the 2022 growing season had an estimated return period of approximately 60 years.
- Most droughts resulted from extended periods of below average precipitation, while some developed and intensified rapidly due to co-occurrence with heatwaves (flash droughts). Several compound drought and heatwave events have also been observed in recent years.
- The intensity of drought conditions on shorter timescales (1 to 2 months) has been slightly increasing with time since 1970. On average, the number of dry months and severely dry months has also increased in the last few decades in the region. The number of heatwaves, the number of heatwave days and the maximum heatwave magnitude have been increasing across the case study area since 1950. As a result, the number and the magnitude of compound drought and heatwave events also show an increase at certain locations.
- In the future, both droughts and heatwaves are expected to become more severe and more frequent with respect to current conditions (1991–2020) under all global warming levels. The frequency of compound drought and heatwave events is expected to increase by between 1 to 5 events annually under global warming level of 3 to 4 °C, corresponding to a relative increase from

15 to over 100 %. Regardless of the global warming level, the intensity of future events is expected to increase by 40 % to 150 %.

- The probability of occurrence of individual drought and heatwave events, as well as the occurrence of compound drought and heatwave events are expected to increase in the future. A compound drought and heatwave event as extreme as the 1-in-50-year event in 1991–2020 is projected to become up to 6–8 times as likely under a global warming level of 3 °C and up to 12–13.5 times as likely under a global warming level of 4 °C.

## GROUNDWATER DROUGHT

- A statistically significant decreasing trend in groundwater levels was observed for every month from April to July in the period 1981–2023.
- A comparison of the soil water deficit index for two 30-year periods, 1971–2000 and 1991–2020, shows that there were more drought days and more consecutive drought days in the period 1991–2020.
- In the period 1971–2023, according to the data of groundwater recharge, there were severe droughts (95<sup>th</sup> percentile) between March and August in the years 1993 and 2022. In the same time span, the following years had moderate droughts (75<sup>th</sup> percentile): 1997, 2003, 2011, 2012, 2015, and 2017.
- It is expected that future groundwater recharge values (March–August) will be similar to the average values from the reference period 1991–2020, due to winter and spring precipitation.

# PAST EXTREME EVENTS IN FOCUS



## DROUGHT INTENSIFIED BY HEATWAVES IN THE 2022 GROWING SEASON

Summer of 2022 in Slovenia was characterised by a persistent lack of precipitation, record high temperatures and several heatwaves, which lead to extreme dryness of the topsoil layer, particularly in the western part of the country. The months-long precipitation deficit, which lasted almost continuously from January until the beginning of September 2022, ranked 2022 one of the driest years meteorologically in Slovenia. At the beginning of the summer, the conditions already indicated drought at the scale of a natural disaster. A series of heatwaves (the number ranging from 1 to 4, depending on the location) that occurred from the second half of June to the end of August, led to a long period of severe heat stress and, in combination with a lack of precipitation and dried-out soils, strongly affected ecosystems. At the end of July, the natural vegetation was already showing signs of yellowing and leaf fall typical

of autumn. In July, high fire risk was also declared for the entire country and the most extensive wildfire in Slovenia broke out in its western part. In general, the western and central Slovenia were more affected by topsoil drought, while it was less pronounced in the east of the country. In terms of duration and severity, the topsoil drought in 2022 ranks among the most extreme in Slovenia. It affected 23,570 people in 211 municipalities. The final economic damage was estimated at 148 million euros, exceeding 30 % of normal annual agricultural production, meaning that the 2022 drought was indeed declared a national disaster. In addition to agriculture, natural systems and other key socio-economic sectors, such as energy and river transport were also affected. Groundwater drought was observed as well, resulting in municipalities and utility companies throughout Slovenia advising people to conserve water, and firefighters delivering drinking water to users (including livestock) without access to it, especially to settlements at higher altitudes.



**FIGURE 1:** Maize harvest in 2022 was affected, as maize is very susceptible to drought.

# DEFINITION OF METEOROLOGICAL AND GROUNDWATER EXTREMES



## METEOROLOGICAL AND TOPSOIL DROUGHT

The **Standardized Precipitation Index (SPI)** gives a measure of what a certain amount of precipitation over a chosen timescale (monthly to multi-monthly) means in relation to the expected amount of precipitation for this timescale for any given location. Values of the SPI index around 0 (between -1 and 1) represent the normal expected precipitation amount conditions over a chosen timescale based on the long-term average (1991–2020). Values above 1 represent precipitation surplus – wet conditions, and values below -1 precipitation deficit – dry conditions (-1.5 to -1 moderately dry, -2 to -1.5 severely dry, below -2 extremely dry).

The **Standardized Precipitation-Evapotranspiration Index (SPEI)** gives a measure of what a certain value of surface water balance (the difference between precipitation and reference evapotranspiration) over a chosen timescale (monthly to multi-monthly) means in relation to the expected value of surface water balance for this timescale for any given location. Values of the SPEI index around 0 (between -1 and 1) represent the normal expected surface water balance conditions over a chosen timescale based on the long-term average (1991–2020). Values above 1 represent surface water balance surplus – wet conditions, and values below -1 surface water balance deficit – dry conditions (-1.5 to -1 moderately dry, -2 to -1.5 severely dry, below -2 extremely dry).

The **Evaporative Demand Drought Index (EDDI)** examines how anomalous the atmospheric evaporative demand ( $E_0$ ; also known as “the thirst of the atmosphere”) is for a given location and for a timescale of interest relative to the long-term average (1991–2020). Similarly as SPI and SPEI, EDDI is multi-scalar, meaning

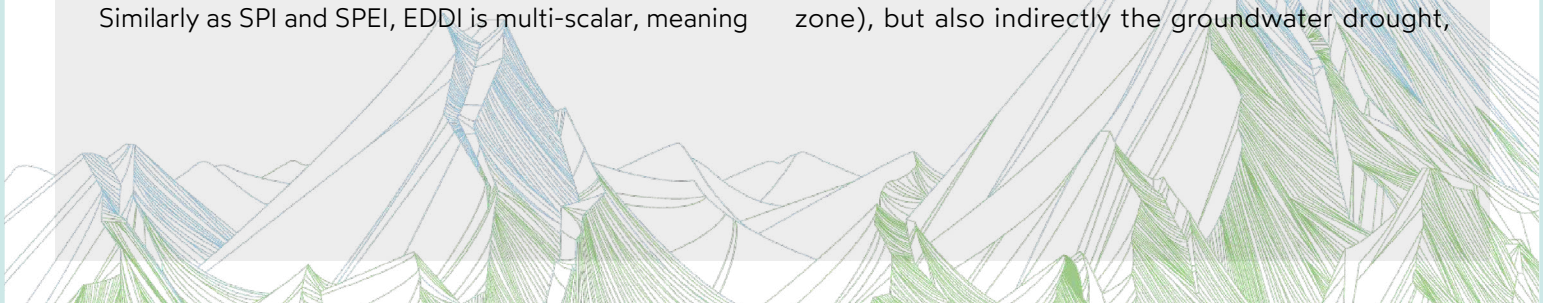
that the timescale can vary to capture drying dynamics that operate at different timescales. Values around 0 (between -1 and 1) represent the normal expected conditions, values above 1 dry conditions (-1.5 to -1 moderately dry, -2 to -1.5 severely dry, below -2 extremely dry), and values below -1 wet conditions.

The **90-day surface water balance** is defined as the difference between precipitation and evapotranspiration accumulation over a period of 90 days. By comparing the value with historical information over the same period, namely 90-day accumulations in the reference period 1991–2020, a percentile value can be assigned to it. The 90-day period is used since it corresponds to a period of 3 months which is the length of meteorological season.

## HYDROLOGICAL DROUGHT IN GROUNDWATER

The **net groundwater recharge (Q<sub>rn</sub>)** is determined in the mGROWA model by separating the calculated total runoff into the components of direct runoff and baseflow. Groundwater recharge designates the volume of water, which percolates through the unsaturated zone and reaches the aquifer. Hence, groundwater recharge occurs at the top of the water saturated zone, i.e. the upper aquifer (Andjelov et al., 2016). Simulated groundwater recharge levels are presented as long-term annual averages and as long-term monthly values in order to indicate the seasonal fluctuation of groundwater recharge rates (Herrmann et al., 2015). Q<sub>rn</sub> is given in millimetres (mm).

The **Soil Water Deficit (SWD)** from the mGROWA model index primarily indicates the drought in the soil (root zone), but also indirectly the groundwater drought,



because soil drought and groundwater recharge are interdependent and connected. This index is suitable because it is calculated for the entire area of Slovenia. It shows the soil drought conditions throughout Slovenia (not only on agricultural land) and is therefore useful also as a complementary index of watershed area water infiltration conditions. **SWD60** shows the number of days in the growing season of the year with a water deficit above 60 % – this threshold is considered as a medium soil drought value. On a day with the SWD index greater than 60, the plant has only 40 % of the water theoretically required for normal plant-respiration process available in the soil. Two indicators are highlighted: **ndSWD** shows the number of days in a period with an exceeded degree of drought using the SWD60 index, and **mdSWD** shows the maximum number of consecutive drought days using SWD60. A percentage is used to describe the deficit level (Strgar and Frantar, 2019).

The **Standardised Groundwater Level Index (SGI)** represents a measure of what a certain value of the level of the groundwater level means in relation to the normal or expected value. The SGI is the statistically standardized deviation of the average monthly groundwater level from the long-term average (1991–2020). Negative values of the SGI index indicate the degree of groundwater drought, which is characterized by a period of water deficit in the aquifer relative to normal conditions. The groundwater drought indicator in intergranular aquifers is based on an assessment of the intensity and spatial distribution of the monthly standardised groundwater level index for individual hydrological years (1<sup>st</sup> November–31<sup>st</sup> October). The indicator defines 3 intensities of drought: mild drought:  $-1 < SGI < 0$  (D0 drought category according to USD model), moderate drought:  $-1.5 < SGI < -1$  (drought category D1 according to USD model); severe drought:  $-2 < SGI < -1.5$  (drought category D2 according to USD model); extreme drought:  $SGI < -2$  (D3 drought category according to USD model) (Pavlič, 2024).

## HEATWAVES

A **heatwave (HW)** event corresponds to three or more consecutive days with maximum daily temperatures above the 95<sup>th</sup> percentile of the reference period (1991–2020), which has been widely utilised to identify heatwave events. Heatwave magnitude is defined as the sum of the differences between the daily maximum temperature and the threshold temperature (95<sup>th</sup> percentile) for all heatwave days:

$$HW_{magnitude} = \sum_1^N sum(T_{max} - T_{threshold})$$

where  $N$  is the length of the heatwave in days. In other words, the magnitude represents the accumulated excess temperature during a heatwave.

## COMPOUND DROUGHT AND HEATWAVE

Compound drought and heatwave events (CDHW) can be analysed from a qualitative and quantitative perspective using various combinations of different drought (e.g., SPI, SPEI and EDDI) and heatwave indicators. The selected approach is based on Zhang et al. (2022), who define CDHW through a combination of SPEI-3 and maximum daily temperature. In our case, compound events for shorter SPEI time scales (SPEI-1 and SPEI-2) are also considered.

**Magnitude of compound drought and heatwave (CDHW)** event can be described by combining drought and heatwave conditions and is defined as:

$$M = \frac{1}{N} \sum_{n=1}^N (T_{max_i} - thre) * |SPEI_i|$$

where  $M$  is the magnitude of compound event,  $N$  is the total days of compound event,  $T_{max_i}$  is the maximum temperature of the  $n$  day of compound event,  $thre$  is the temperature threshold, which is the 95<sup>th</sup> percentile of the reference period (1991–2020) and  $SPEI_i$  is the value of SPEI(1-3) during the month of the  $n$  day of compound events (adapted from Zhang et al., 2022).



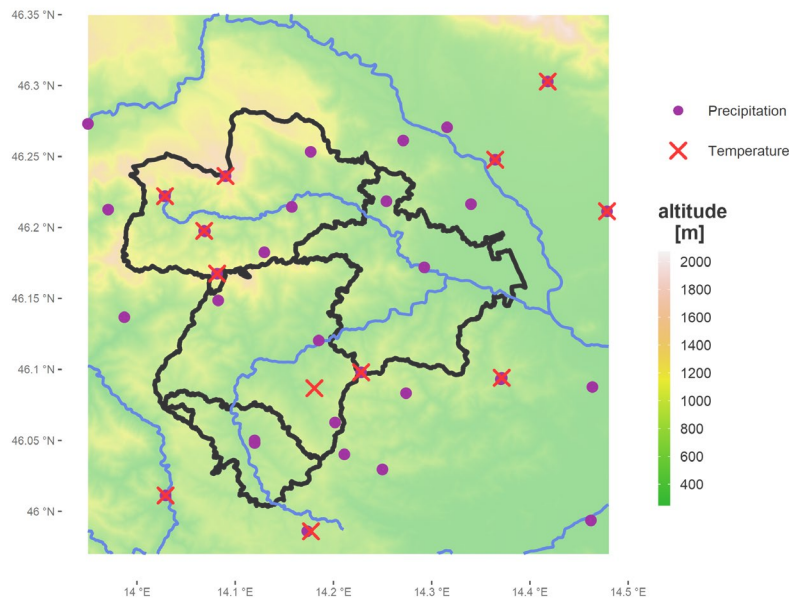


**FIGURE 2:** Precipitation and temperature stations in the greater Sora catchment region. Purple dots denote 24 precipitation stations and red crosses denote 12 temperature stations. The borders of municipalities of the Sora catchment are marked with a black line.

## METEOROLOGICAL DATA

For the case study area of the Sora catchment in Gorenjska, observations of daily precipitation at 31 stations, maximum daily temperature at 12 stations (**FIGURE 2**) and reference evapotranspiration at 1 station (calculated from measurements using the Penman-Monteith method for J.P. Airport) are used for the analysis of drought and heatwave events in the period from 1970 to August 2023 (from 1950 for heatwaves). In addition, we used spatially interpolated monthly values of reference evapotranspiration to obtain SPEI and EDDI for 30 precipitation stations where daily reference evapotranspiration was not available. All datasets have undergone homogenization and missing data were interpolated from neighbouring stations.

When analysing station observations, it is important to consider that these can be affected by uncertainties, especially in areas characterised by complex orography. In particular, precipitation amounts at high-elevation sites can be underestimated, especially during episodes of high wind speeds and snowfall.

The analysis of future changes in frequency and intensity of drought, heatwaves and compound drought and heatwave events is based on national projections of daily precipitation, maximum temperature and reference evapotranspiration (calculated from a set of meteorological parameters) with a resolution of 12 km, which were bias-adjusted from EURO-CORDEX model simulations (**TABLE 1**) according to observations in the period 1981–2010 (Bertalanč et al., 2018). The changes

**TABLE 1:** List of bias-adjusted EURO-CORDEX model simulations used for evaluation of projected changes in drought, heatwaves and compound drought and heatwave events in the Sora catchment.

	Global Climate Model	Regional Climate Model (Institute)
1	EC-EARTH	HIRHAM5 (DMI)
2	HadGEM2-ES	RACMO22E (KNMI)
3	CNRM-CM5-LR	CCLM4-8-17 (CLMcom)
4	IPSL-CM5A-MR	WRF331F (IPSL)
5	MPI-ESM-LR	CCLM4-8-17 (CLMcom)
6	MPI-ESM-LR	RCA4 (SMHI)

are examined for four global warming levels relative to the pre-industrial period (1850–1900), namely 1.5 °C (representing very near future conditions), 2 °C, 3 °C and 4 °C and shown as deviations from the reference period 1991–2020.

It is important to note that station observations and model simulations are not directly comparable, even after the bias-adjustment procedure, which increases the overall accuracy of the model fields but does not increase the spatial scales resolved. The coarser spatial resolution of the model simulations therefore limits the representation of features at the local scale, especially in orographically-complex regions.

## GROUNDWATER DATA

The monthly net groundwater recharge ( $Q_{rn}$ ) and the soil water deficit (SWD60) are output data from mGROWA model. Data for the period 1971–2023 were used to analyse groundwater drought in the past, while for the future, projections of net groundwater recharge ( $Q_{rn}$ )

from March to August for the period 1981–2100 were used. In order to verify the results of the mGROWA model, 4 control points were selected in the watershed area. The selection was based on information from interviews with experts about local water resources and analysis of water reimbursements from 2022.

The SGI index is calculated from groundwater level data, which is monitored at the Sveti Duh station in the Sorško polje area in addition to the drought conditions. In the analysis of the groundwater levels in the Sorško polje aquifer due to artificial influences of the Mavčiče hydroelectric power plant, only the measuring station Sveti Duh is considered since it is not influenced by the dam. It is located on the western edge of the aquifer. The Mavčiče hydroelectric power plant significantly contributed to the rise in groundwater levels at other locations of the Sorško polje aquifer. The Sveti Duh station and the HPP Mavčiče are also shown on the map (**FIGURE 3**). The SGI values at all measurement points in Slovenia have not yet been calculated based on climate scenarios until end of the 21<sup>st</sup> century.

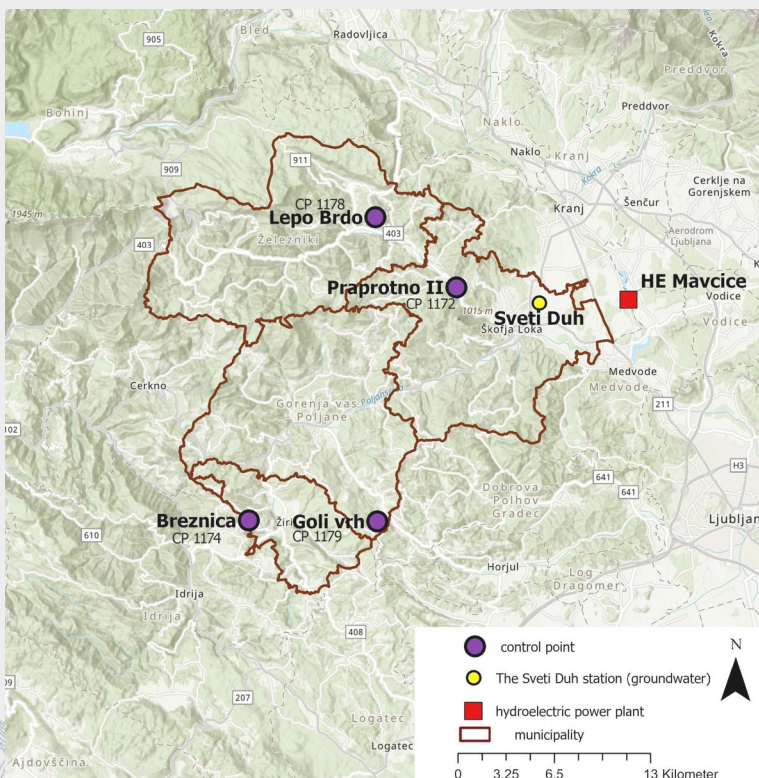


**FIGURE 3:** Map of control points, the Sveti Duh station and the hydroelectric power plant Mavčiče.

# TYPICAL SYNOPTIC SITUATION LEADING TO THE EXTREME EVENT



## SYNOPTIC SITUATION: DROUGHT 2022

In 2022 a significant drought affected Europe, and Slovenia alike. During the period from May to July, high mid-tropospheric pressure anomalies have been observed over most of Europe, ranking among the highest since 1950 for these months, particularly in western, southern and central Europe. These nearly stationary atmospheric circulation patterns are typically associated with both heatwaves and droughts during the summer months in Europe, as they block or redirect the migratory cyclones that normally bring moist and cool air. Persistent high-pressure conditions were observed from late spring to late summer, enhancing pre-existing drought conditions, as a persistent lack of precipitation was observed from winter 2021/22 onwards. On an annual scale, the surface soil moisture

in Europe was the second lowest in the last 50 years (Copernicus C3S, 2023). Higher-than-average temperatures and a sequence of heatwaves that started in spring and continued throughout summer sustained and enhanced drier-than-average conditions.

The mean sea level pressure data from ERA5 reanalysis yields mainly anti-cyclonic GWTs ('Gross-Wetter-Type'; a circulation type classification) over a prolonged time period, which is the cause for overwhelming subsidence and generally warm and dry conditions. If these circulation patterns hold over longer periods of times and are not interrupted by longer lasting cyclonic circulation patterns, drought conditions increase. Notably in anticyclonic GWTs for Central Europe, cyclonic pressure systems are located either in Northern Europe, or over the Atlantic and then may be deflected by quasi-stationary ridges, which can lead to prolonged drought



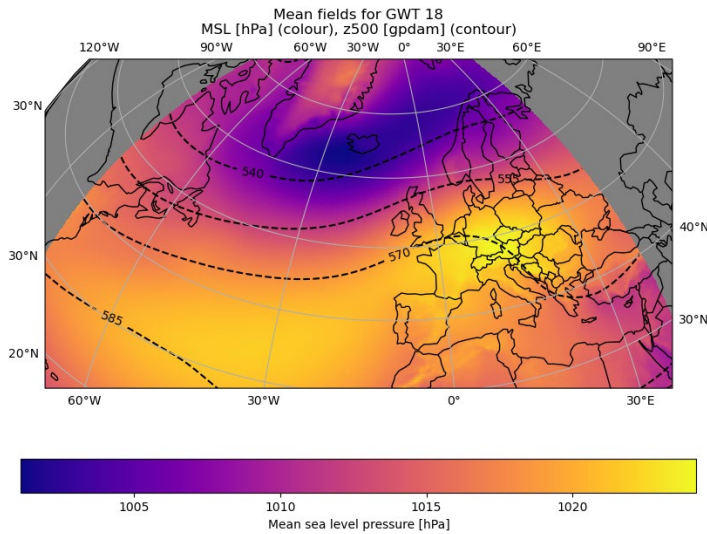


**FIGURE 4:** GWT 18 is characterized by an extensive high-pressure system over Central Europe, causing dry and warm conditions. Mean sea level pressure is shown in colours, 500 hPa geopotential as contours.

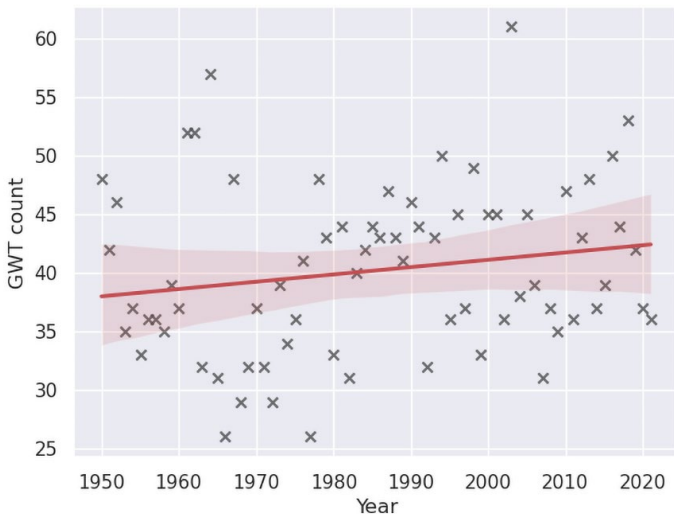
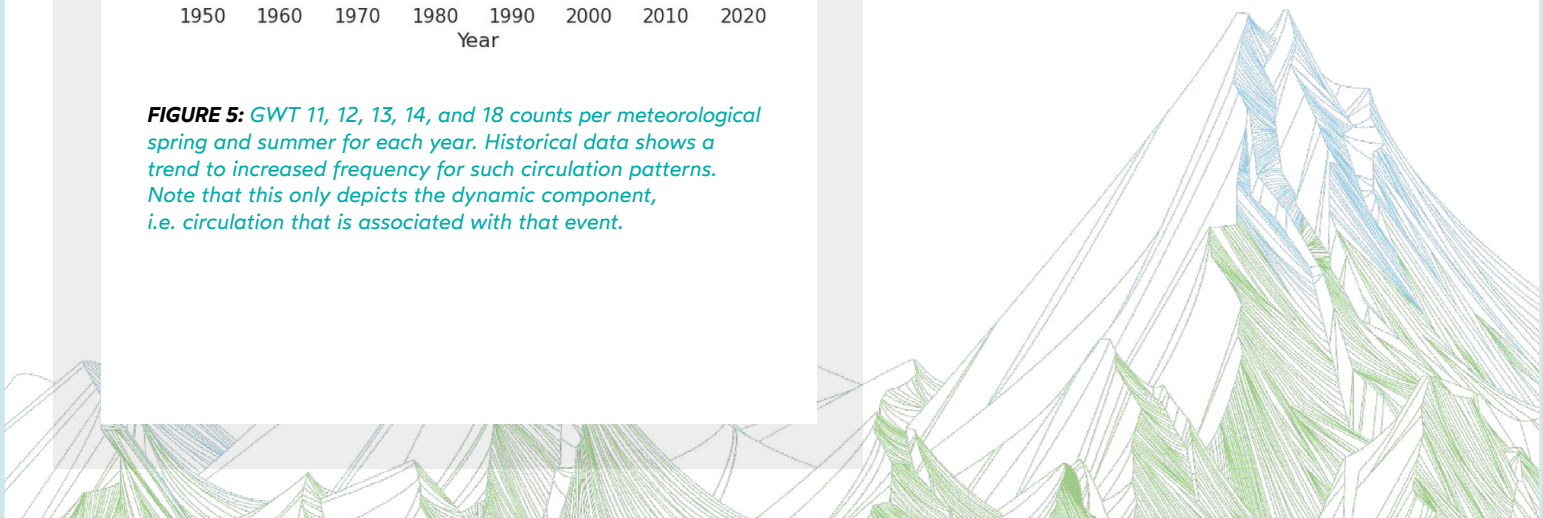


**FIGURE 5:** GWT 11, 12, 13, 14, and 18 counts per meteorological spring and summer for each year. Historical data shows a trend to increased frequency for such circulation patterns. Note that this only depicts the dynamic component, i.e. circulation that is associated with that event.

conditions, particularly in Central, Southern and Southeastern Europe. Furthermore, as visible in **FIGURE 4** for GWT 18, the Alps reside in front of the ridge axis and hence experience strengthened subsidence. Depending on the exact location of the ridge, air may also experience prolonged drying over continental areas, which in particular is again the case for GWT 18. Generally, circulation patterns that reinforce drought are found to be GWT 11, 12, 13, 14, and 18. The historical trend can be seen in **FIGURE 5**. An increasing trend for the frequency of those circulation patterns in meteorological spring (March to May) and summer (June to August) can be seen, with a decadal minimum around 1970.

Note that GWTs only capture the large-scale circulation of the weather situation and serve as preconditioning for extreme weather events. However, the existence of a specific GWT class alone does not entail extreme weather events all the time. There are more fine-grained details and thermodynamic components that also play a role in any specific weather situations. Nevertheless, the GWT analysis allows to estimate large-scale circulation changes and therefore changes to the preconditioning relevant for extreme weather events.



# CHARACTERISTICS OF EXTREME EVENTS IN THE PAST



## TOPSOIL DROUGHT: FREQUENCY, INTENSITY AND PROBABILITY OF OCCURRENCE IN THE PERIOD 1970–2023

Different drought indices were used for the analysis of past drought events, namely SPI, SPEI and EDDI. The results are reported based on SPEI, which combines both key meteorological variables influencing drought conditions – precipitation and reference evapotranspiration. Over the last two decades, the most

severe droughts in the case study area have been recorded in the 2003 growing season, the summer 2013 and the 2022 growing season, indicating severely to extremely dry conditions based on SPEI over different timescales, while moderately dry conditions have occurred more frequently (**FIGURE 6**). During the summer 2022, the recorded SPEI values were below  $-2$ , indicating extremely dry conditions. Based on the 90-day surface water balance for summer (similar to SPEI-3 for August, but given in absolute values) at

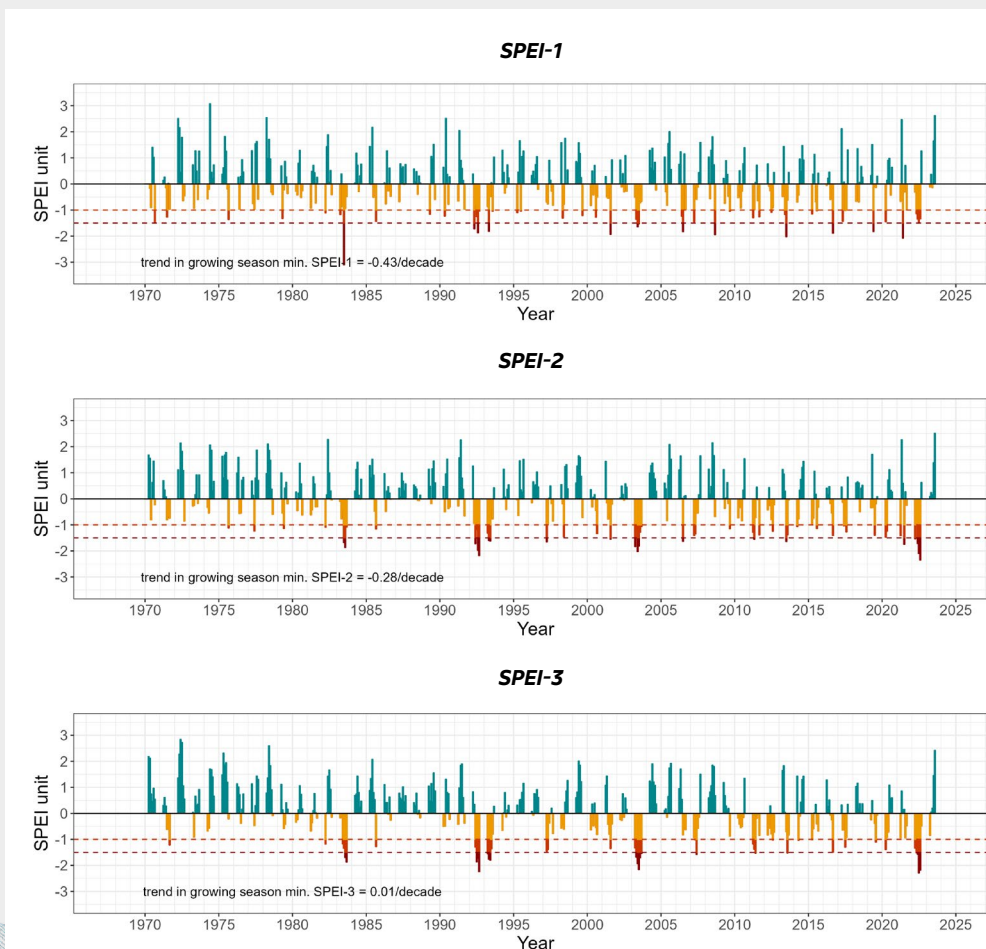


**FIGURE 6:** Timeline of SPEI in growing season months (from April to September) on a timescale of 1 month (top), 2 months (middle) and 3 months (bottom) in the period 1970–August 2023 for J.P. Airport station. Dry and severely dry months are indicated by bright and dark red respectively. Similar timelines are observed for other stations in the region.



J.P. Airport, drought conditions recorded in summer 2022 fall below the 0<sup>th</sup> percentile of the 1991–2020 reference period. The return period of such drought conditions is estimated at approximately 60 years (at 90 % confidence interval, the lower bound is estimated at 25 years).

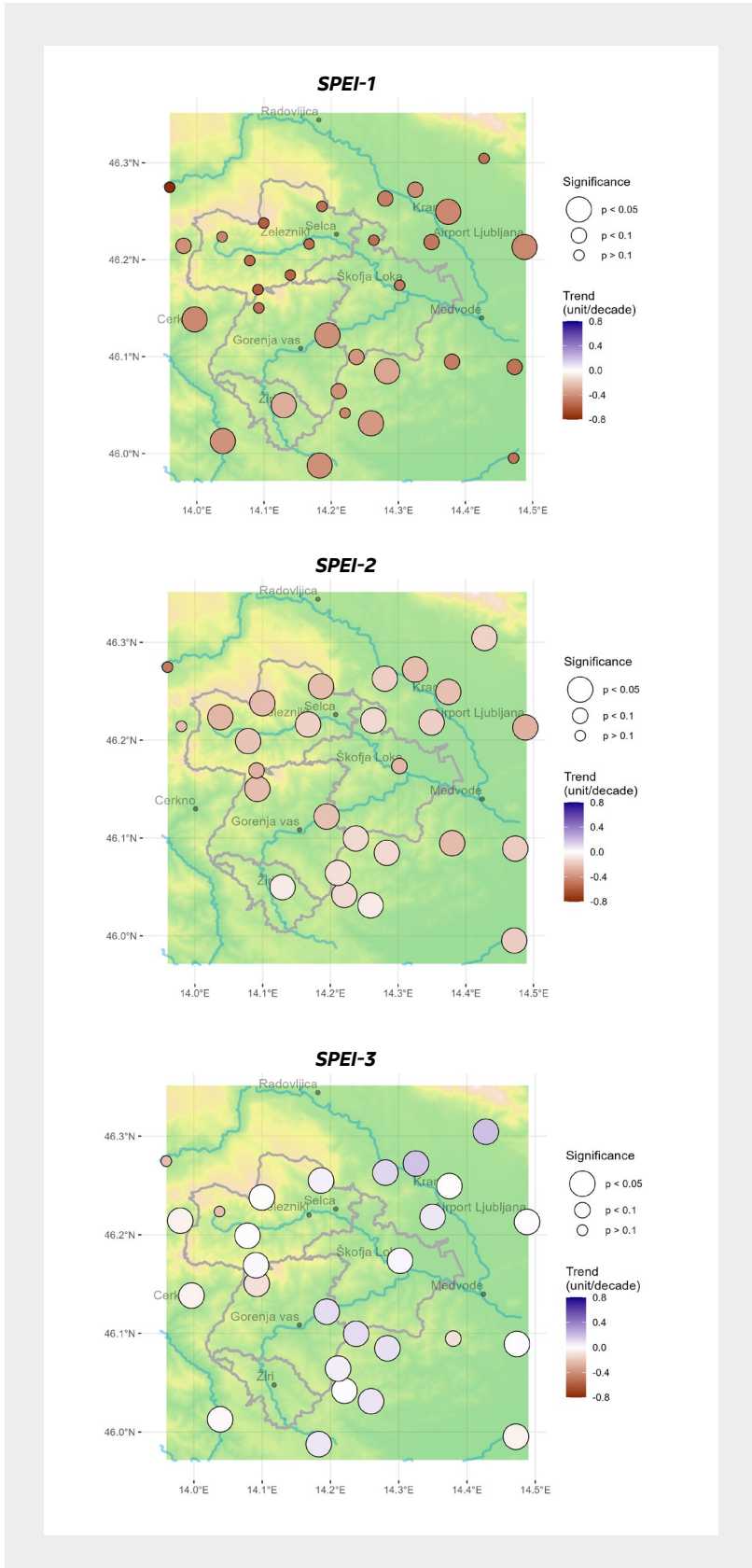
There are no statistically significant trends in the number of dry months in a growing season in the period 1970–August 2023. However, when comparing the number of dry months and severely dry months in two subsequent 30-year periods, 1971–2000 and

1991–2020, the number of months with SPEI values equal to and below  $-1$  and  $-1.5$  respectively increased on all analysed stations. In the latter period, we recorded 10–18 more dry months and 6–7.5 more severely dry months on average in the case study area, depending on the SPEI timescale (**TABLE 2**). The frequency of at least moderately dry months and at least severely dry months thus appears to be increasing with time.

The minimum value of SPEI in a growing season (the months from April to September), which can be related to the intensity of topsoil drought conditions, shows

**TABLE 2:** The total number of dry months and severely dry months in a growing season in the period 1971–2000 and 1991–2020 based on SPEI on a timescale of 1 month (SPEI-1), 2 months (SPEI-2) and 3 months (SPEI-3), averaged over all stations in the case study area (including the range in the number of dry months over all stations given in brackets). Dry months are defined as months with SPEI values equal to or below  $-1$ , while severely dry months are defined as months with SPEI values equal to or below  $-1.5$ .

	1971–2000		1991–2020		Difference	
	No. of dry months (SPEI $\leq$ -1.0)	No. of severely dry months (SPEI $\leq$ -1.5)	No. of dry months (SPEI $\leq$ -1.0)	No. of severely dry months (SPEI $\leq$ -1.5)	No. of dry months (SPEI $\leq$ -1.0)	No. of severely dry months (SPEI $\leq$ -1.5)
<b>SPEI-1</b>	<b>20.8</b> (14–35)	<b>7.0</b> (3–12)	<b>31</b> (26–34)	<b>13.9</b> (11–17)	<b>10.2</b> (-3–18)	<b>6.9</b> (3–10)
<b>SPEI-2</b>	<b>15.7</b> (10–26)	<b>4.9</b> (1–12)	<b>33.4</b> (28–39)	<b>12.4</b> (8–16)	<b>17.7</b> (10–24)	<b>7.5</b> (0–13)
<b>SPEI-3</b>	<b>16.3</b> (12–22)	<b>7.0</b> (3–12)	<b>32.2</b> (28–37)	<b>13.1</b> (10–17)	<b>15.9</b> (9–22)	<b>6.1</b> (1–10)



statistically significant negative trend for timescales from 1 to 2 months (SPEI-1, SPEI-2) for a number of stations, and statistically significant trend in both directions for a timescale of 3 months (**FIGURE 7, TABLE 3**). The intensity of drought conditions on shorter timescales has thus been slightly increasing with time, but due to greater variability on shorter timescales, the trends for SPEI-1 are statistically significant for a smaller number of stations compared to SPEI-2 or SPEI-3. The trend in SPEI-3 is generally less pronounced than the trend on shorter timescales, but statistically significant across the case study area.

**FIGURE 7:** Linear trend in growing season minimum SPEI on a timescale of 1 month (left), 2 months (middle) and 3 months (right) at respective stations in the period 1970–2023, including statistical significance of trends.

**TABLE 3:** Linear trend in growing season minimum SPEI on a timescale of 1 month (SPEI-1), 2 months (SPEI-2) and 3 months (SPEI-3), averaged over all stations in the case study area. The lower bound corresponds to the minimum trend and the upper bound to the maximum trend over all stations.

	Trend/decade	Lower bound	Upper bound
Minimum SPEI-1	-0.41	-0.51	-0.29
Minimum SPEI-2	-0.18	-0.28	-0.07
Minimum SPEI-3	0.04	-0.11	0.19

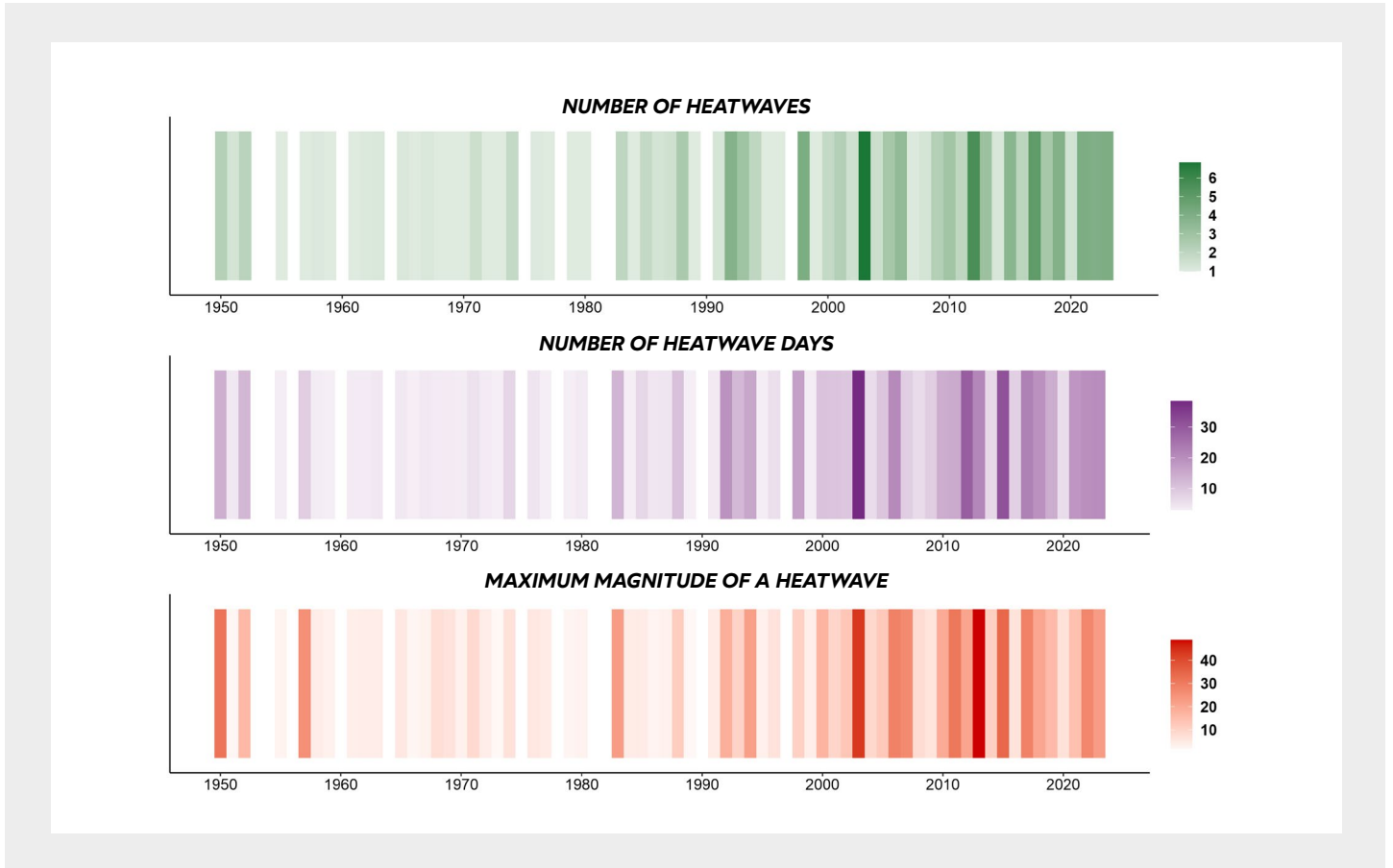


**FIGURE 8:** Number of heatwaves, number of heatwave days and maximum magnitude of a heatwave, averaged over all stations in the case study area, in the period 1950–2023.

### HEATWAVES: FREQUENCY, INTENSITY AND PROBABILITY OF OCCURRENCE IN THE PERIOD 1950–2023

The years 2003 and 2013 were the most extreme in terms of heatwaves in the case study area (**FIGURE 8**). In 2003, we observed 7 or more heatwaves, with the longest one lasting from 10 up to 23 days. We also recorded the highest number of heatwave days, which was between 34 and 46 days. However, in terms of

heatwave magnitude, the 2013 heatwave was the most extreme. The maximum magnitude of the 2013 heatwave was over 50 at half of the stations, whereas in 2003 the magnitude was below 50 at all stations. The year 2022 ranked 7<sup>th</sup> on the record in the number of heatwaves and 8<sup>th</sup> in the number of heatwave days, whereas the maximum magnitude was within 23 and 32 (8<sup>th</sup>). While the year 2022 was not among the top years on the record in extreme heat conditions, heatwaves concurrent with droughts intensified their individual impacts.

**TABLE 4:** Linear trend in the number of heatwaves, the number of heatwave days and the maximum magnitude averaged over all stations in the case study area. The lower bound corresponds to the minimum trend and the upper bound to the maximum trend over all stations.

	Trend/decade	Lower bound	Upper bound
Number of heatwaves	0.3	0.1	0.5
Number of heatwave days	2.2	1.1	3.4
Maximum magnitude of heatwave	2.4	1.1	4.2

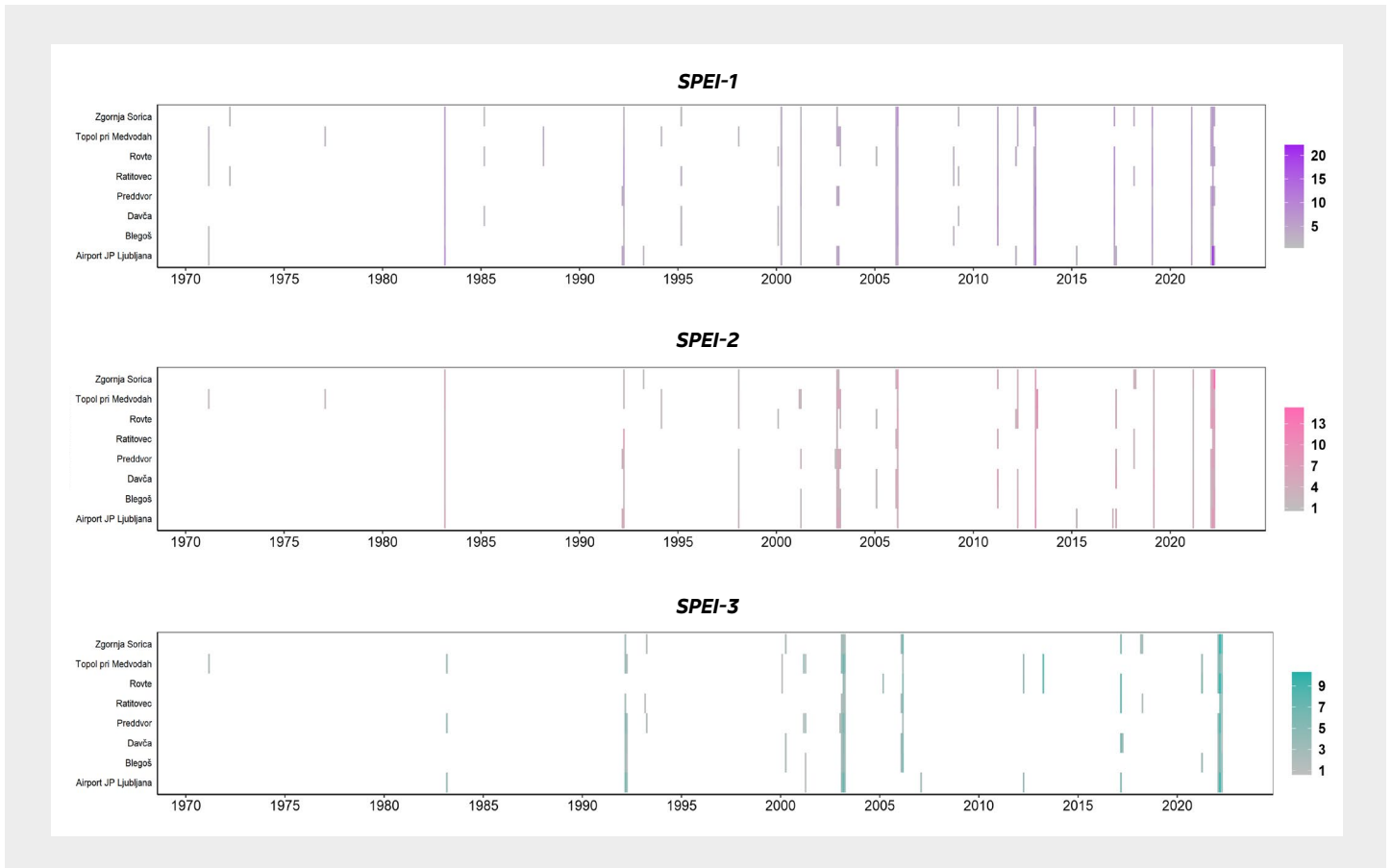


**FIGURE 9:** Magnitude of compound drought and heatwave events for different SPEI timescales in the period 1970–2023.

The number of heatwaves, the number of heatwave days and the maximum heatwave magnitude have been increasing across the case study area since 1950, as indicated by statistically significant positive linear trends in the period 1950–2023 (**TABLE 4**).

The strongest heatwave in 2013 had a magnitude between 43 and 55 at different stations, which is estimated to have a 22 to 38-year return period. In the summer 2022 the strongest heatwaves had maximum magnitudes from 23 to 32, which is estimated to have a 5 to 10-year return period. The maximum magnitudes associated with 25-, 50- and 100-year return periods are shown in **TABLE 5**.

## COMPOUND DROUGHT AND HEATWAVE EVENTS: FREQUENCY, INTENSITY AND PROBABILITY OF OCCURRENCE IN THE PERIOD 1970–2023

Several compound drought and heatwave events have been observed in recent years. They are becoming stronger, as indicated by the increasing magnitude over time (stronger colours towards the right of **FIGURE 9**). The high intensity of the compound event in 2022 and 2003 (with the exception of a combination of heatwave and SPEI-1) stands out in particular, as it was detected at all stations in the case study area. In these years, severely to extremely dry conditions led to drought being declared a natural disaster on a national level.

**TABLE 5:** Return values for heatwave magnitude for 25-, 50- and 100-year return periods. The intervals in maximum magnitudes correspond to the range of return values over all stations for different return periods. A linear trend in the location parameter is considered in the estimation; estimates are calculated for the year 2023.

Return period [years]	25	50	100
Maximum magnitude	42–49	48–60	55–73

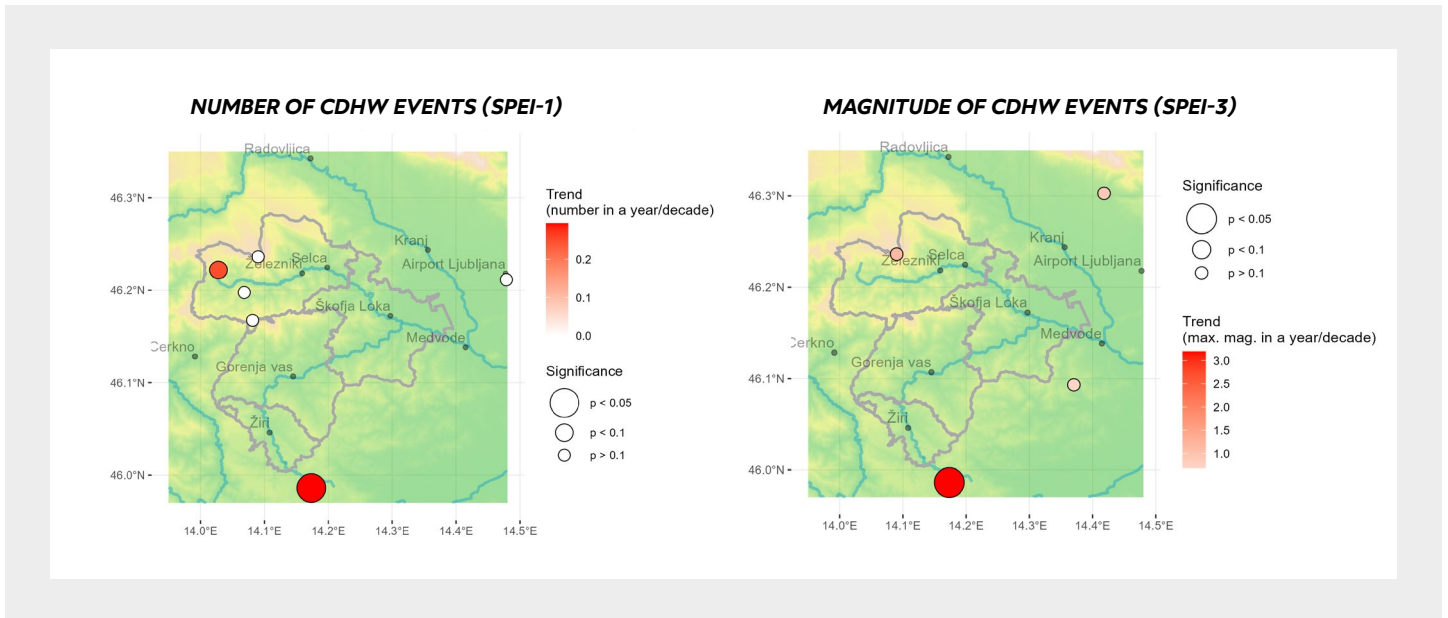


**FIGURE 10:** Linear trend in the number of compound drought and heatwave events based on SPEI-1 (left) and in the magnitude of compound events based on SPEI-3 (right) in the period 1970–2023, including statistical significance of trends. For some stations, trend calculation was not possible due to a low number of compound events.

The analysis of compound events was performed using different indicators of drought (SPI-1, SPI-2, SPI-3, SPEI-1, SPEI-2, SPEI-3 and EDDI) and heatwave in order to examine how different timescales influence the characteristics of the compound event. The conclusions regarding the frequency of compound events are similar for all combinations of indicators. The trend in the number of compound events over time is generally not statistically significant, except for drought indices on a timescale of one month, where the trend in the number of compound events based on SPI-1 and SPEI-1 (**FIGURE 10** left) was positive for two stations in or near the pilot area. The magnitude of compound events is statistically significantly increasing on some stations (**FIGURE 10** right), except for compound events based

on SPEI-2 and EDDI, where no statistically significant trend in magnitude can be observed, however, there is a positive signal (tendency) across the case study area.

The magnitude of the strongest compound drought and heatwave event based on SPEI-3 in 2022 ranged from 5.6 to 10.2 for different stations, which is estimated to have a 33 to 172-year return period. This event was detected at all stations in the case study area. In the summer 2013 the magnitude of compound event was around 8 and was detected at only two stations. In the summer 2003 the magnitude of compound event ranged from 3.5 to 7.7 and was also detected at all stations. The maximum magnitudes associated with 25-, 50- and 100-year return periods are shown in **TABLE 6**.

**TABLE 6:** Return values for magnitude of compound events for 25-, 50- and 100-year return periods. The intervals of maximum magnitude correspond to the range of the return values over all stations for different return periods.

Return period [years]	25	50	100
Maximum magnitude (SPEI-1)	6–9	6–13	7–17
Maximum magnitude (SPEI-2)	6–8	6–9	6–12
Maximum magnitude (SPEI-3)	4–7	5–8	6–13

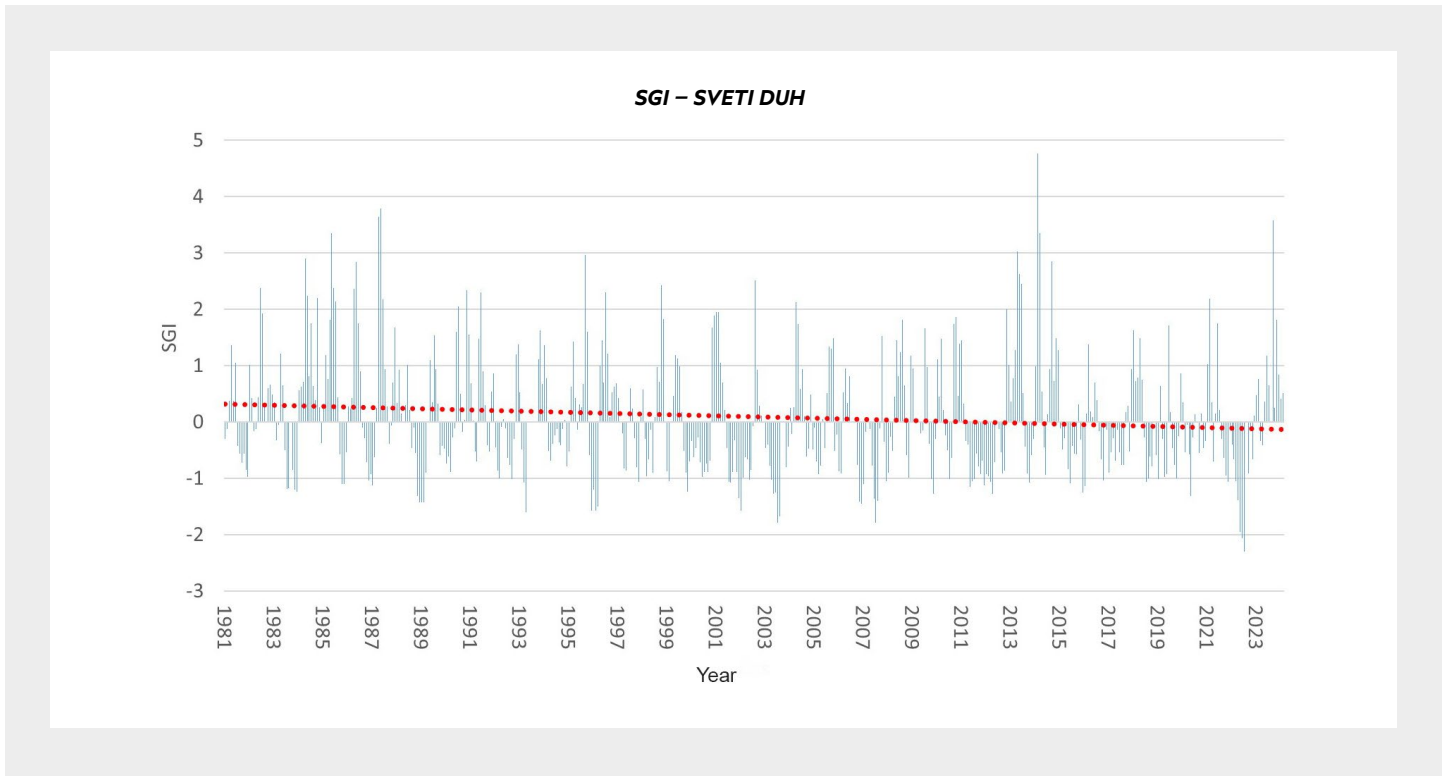


**FIGURE 11:** The course of Standardised Groundwater Level Index (SGI) values at the Sveti Duh measuring station from 1981 to 2023.

**GROUNDWATER DROUGHT:  
FREQUENCY AND INTENSITY IN THE  
PERIOD 1971–2023 OR 1981–2023  
(DEPENDING ON AVAILABLE DATA)**

With a 95 % confidence level, a statistically significant trend of declining monthly SGI values across the analysed measurement period (1981–2023) was found at the Sveti Duh measuring station (**FIGURE 11**).

For the SGI index, the statistical characteristic of the fluctuation trend by month of the year for the period 1981–2023 was analysed at the measuring station Sveti Duh (**FIGURE 12**). For each month from April to July, there

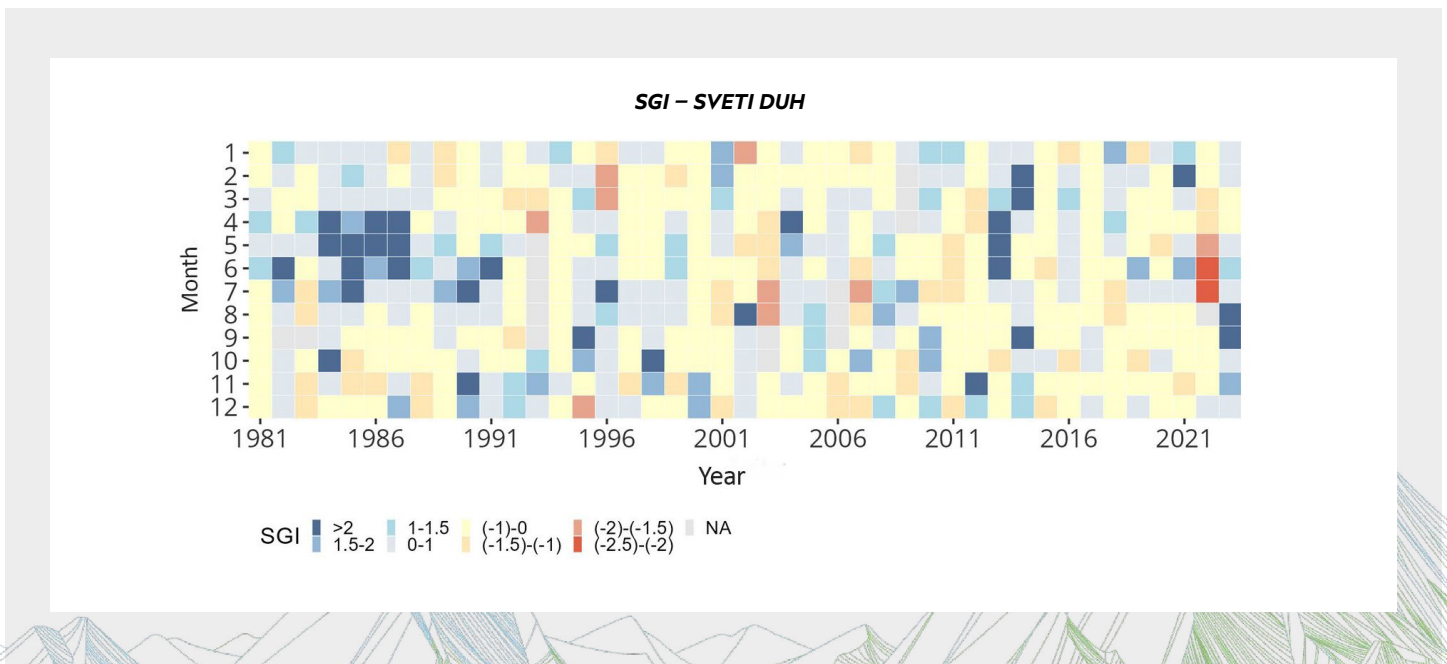


**FIGURE 12:** The course of monthly SGI values at the Sveti Duh measuring station in the period 1981–2023.

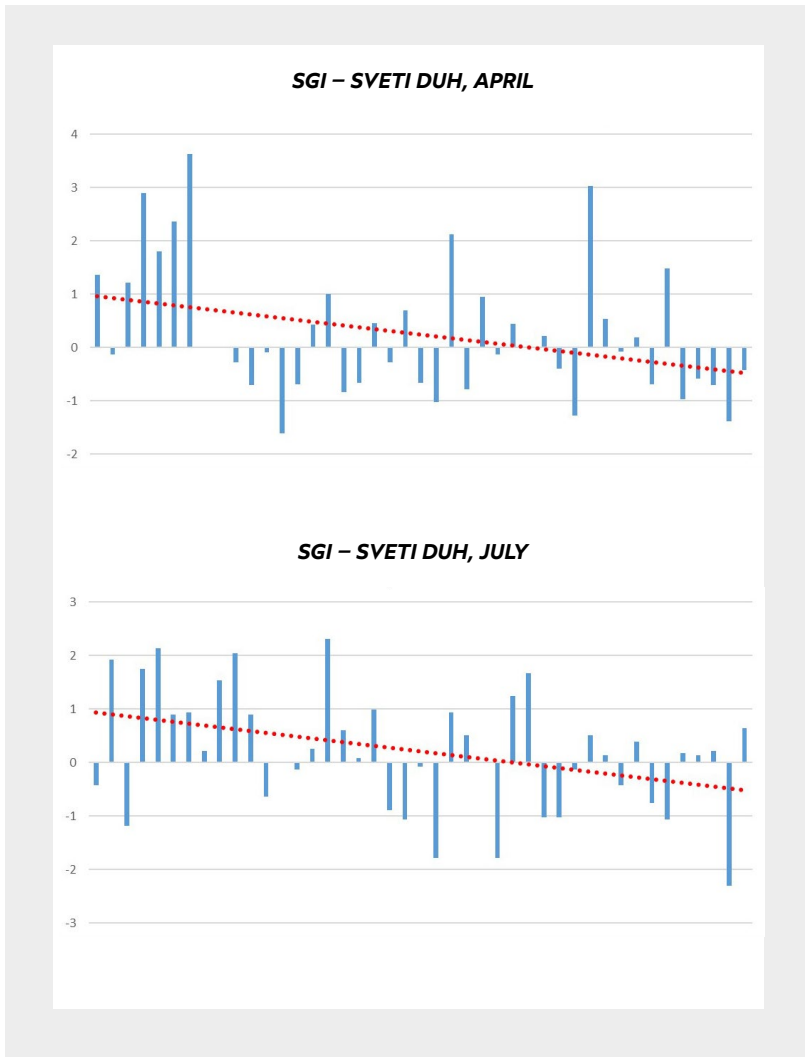


**FIGURE 13:** The linear trend of monthly SGI at the Sveti Duh measuring station in April and July (period 1981–2023).

is a statistically significant decrease in the SGI values (**FIGURE 13**), however, no statistically significant pattern was identified for the remaining months of the year. The SGI at the chosen measuring station increases slightly (statistically insignificantly) in January, February, March, November, and December and decreases in the remaining months (between April and October).

A comparison of the ndSWD60 and mdSWD60 indices (Soil Water Deficit) across two thirty-year periods for four control points in the pilot area is presented in **TABLE 7**. In the period 1991–2020, more drought days (ndSDW60) and more consecutive drought days (mdSWD60) were observed compared to 1971–2000. In both periods, the control point Lepo Brdo was the control point with the most drought days and with the most consecutive drought days. The greatest difference of ndSWD60 values between the two periods were noted at the control point Praprotno II and the greatest difference of mdSWD60 values in the same period were noted at the control point Praprotno II.

**TABLE 7:** The number of drought days (ndSWD60) and the maximum number of consecutive drought days (mdSWD60) per year, averaged over the period 1971–2000 and 1991–2020 at four control points in the case study area, including the difference between the two periods. Drought days are defined as days with SWD60 values above 60. Values show the average number of drought days per year with the minimum and maximum number of days per year in brackets.

Control point	1971–2000		1991–2020		Difference	
	No. of drought days (ndSWD60)	Max. number of consecutive drought days (mdSWD60)	No. of drought days (ndSWD)	Max. number of consecutive drought days (mdSWD60)	No. of drought days (ndSWD)	Max. number of consecutive drought days (mdSWD60)
CP Praprotno II	<b>64.5</b> (12 to 146)	<b>42.5</b>	<b>87</b> (31 to 152)	<b>57.6</b>	<b>22.5</b> (19 to 6)	<b>15.1</b>
CP Breznica	<b>14.4</b> (0 to 72)	<b>10.3</b>	<b>28.2</b> (0 to 127)	<b>20</b>	<b>13.8</b> (0 to 55)	<b>9.7</b>
CP Lepo Brdo	<b>74.8</b> (14 to 168)	<b>52.1</b>	<b>93.1</b> (34 to 168)	<b>61.6</b>	<b>18.3</b> (20 to 0)	<b>9.5</b>
CP Goli vrh	<b>26.5</b> (0 to 81)	<b>15.3</b>	<b>43.5</b> (16 to 116)	<b>22.4</b>	<b>17</b> (16 to 35)	<b>7.1</b>

\* SWD60 shows the number of days in the growing season of the year with a water deficit above 60 %.

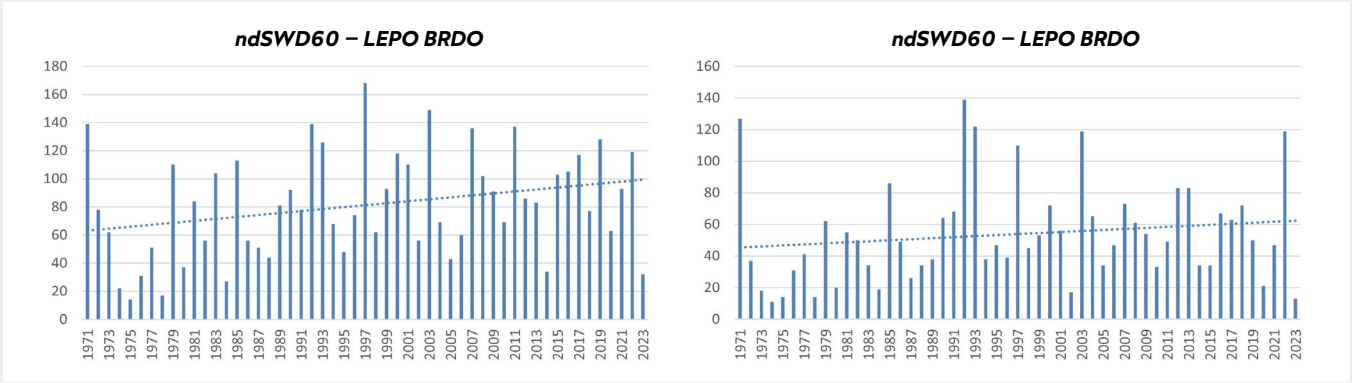


**FIGURE 14:** Soil water deficit (SWD) at the control point Lepo Brdo in the period 1971–2023.

**FIGURE 14** shows the soil water deficit (ndSWD60 and mdSWD60) at the control point Lepo Brdo from 1971 to 2023. Other control points show a similar distribution of years with the most drought days (ndSWD60). The years 1992, 1993, 2003 and 2022 stand out as the years with the most drought days at all control points. At the control points Praprotno II and Lepo Brdo the years 1971, 1997, 2007 and 2011 also stand out. The years with the most consecutive drought days (mdSWD60) at all control points are 2003 and 2022.

All four control points indicate a similar distribution of years with low Q<sub>rn</sub> values. In the period 1971–2023, severe drought conditions (95<sup>th</sup> percentile) were observed from March to August at all four control points in the years 1993 and 2022. Moderate drought conditions (75<sup>th</sup> percentile) occurred within the same

period at all four control points in the years 1997, 2003, 2011, 2012, 2015 and 2017. Additionally, years characterized by moderate drought conditions at three control points include 1994, 2002, 2007 and 2019. **FIGURE 15** shows the seasonal groundwater net recharge (Q<sub>rn</sub>) from March to August for the years 1971–2023 at the control point Praprotno II.

A total of 11 interviews were conducted with experts in water supply management. The participants included representatives of four municipalities (Škofja Loka, Žiri, Železniki and Gorenja vas – Poljane) and managers of public water supply at the local level. The data obtained from these interviews confirm the findings of the mGROWA model. A comparative analysis of the mGROWA model results and the interview data shows consistency in the identified drought years.

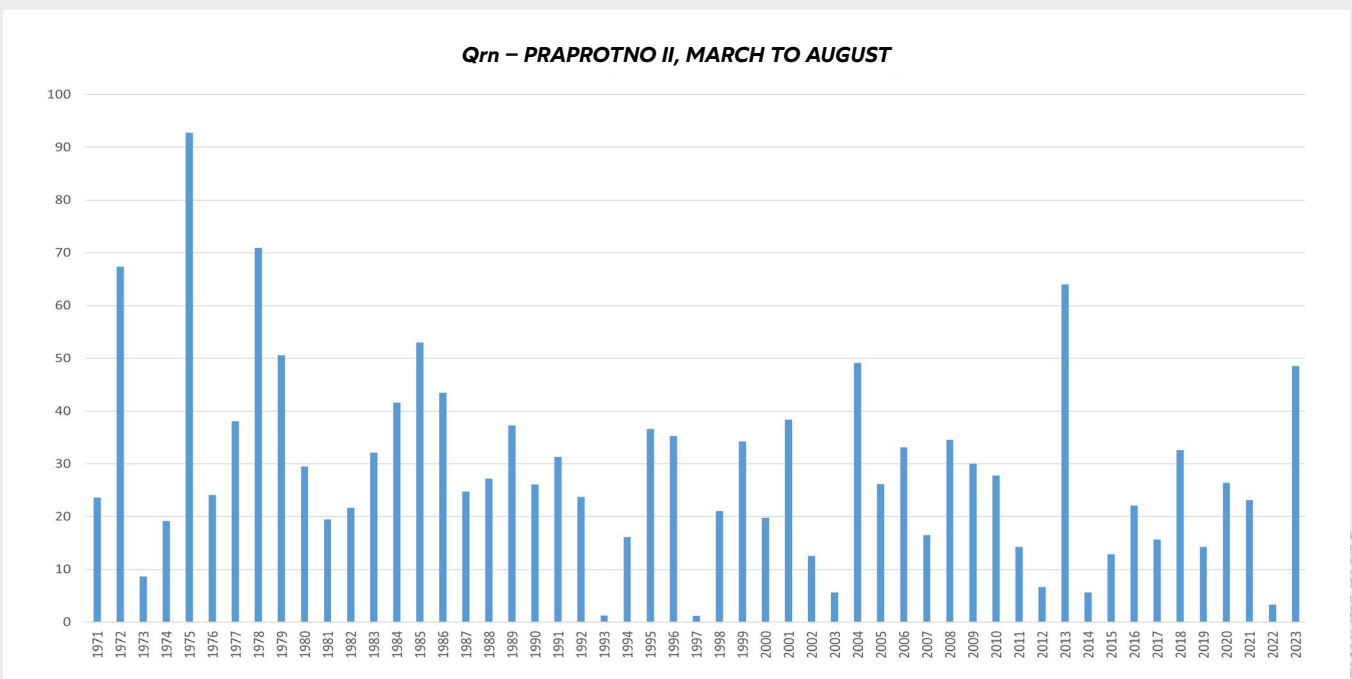


**FIGURE 15:** Groundwater net recharge (Q<sub>rn</sub>) at the control point Praprotno II from March to August.

# WHAT TO EXPECT IN THE FUTURE?



## HOW WILL EXTREME DROUGHT CHANGE?

According to the future projections, a general increase in the number of dry months in a growing season and in the intensity of drought events is expected, regardless of the global warming level (GWL) reached (**FIGURE 16**). The most pronounced changes are expected under the most extreme warming conditions – GWL 4 °C, where the number of dry months and severely dry months is expected to increase by up to a third or half of a month, particularly for SPEI on shorter timescales (1 to 2 months). The growing season minimum SPEI is expected to decrease by approximately 0.5 under

global warming of 4 °C, indicating intensifying drought conditions, while for other global warming levels the change in drought intensity is less pronounced.

The probability of occurrence of extreme drought is expected to increase in the future. A drought event as extreme as the 1-in-50-year event in 1991–2020 (based on 90-day surface water balance in summer) is projected to become up to 2.5 times as likely under GWL 3 °C and 2.9 times as likely under GWL 4 °C. In other words, a 50-year event in the reference period might become a 20-year event in a 3 °C warmer climate and a 17.5-year event in a 4 °C warmer climate.

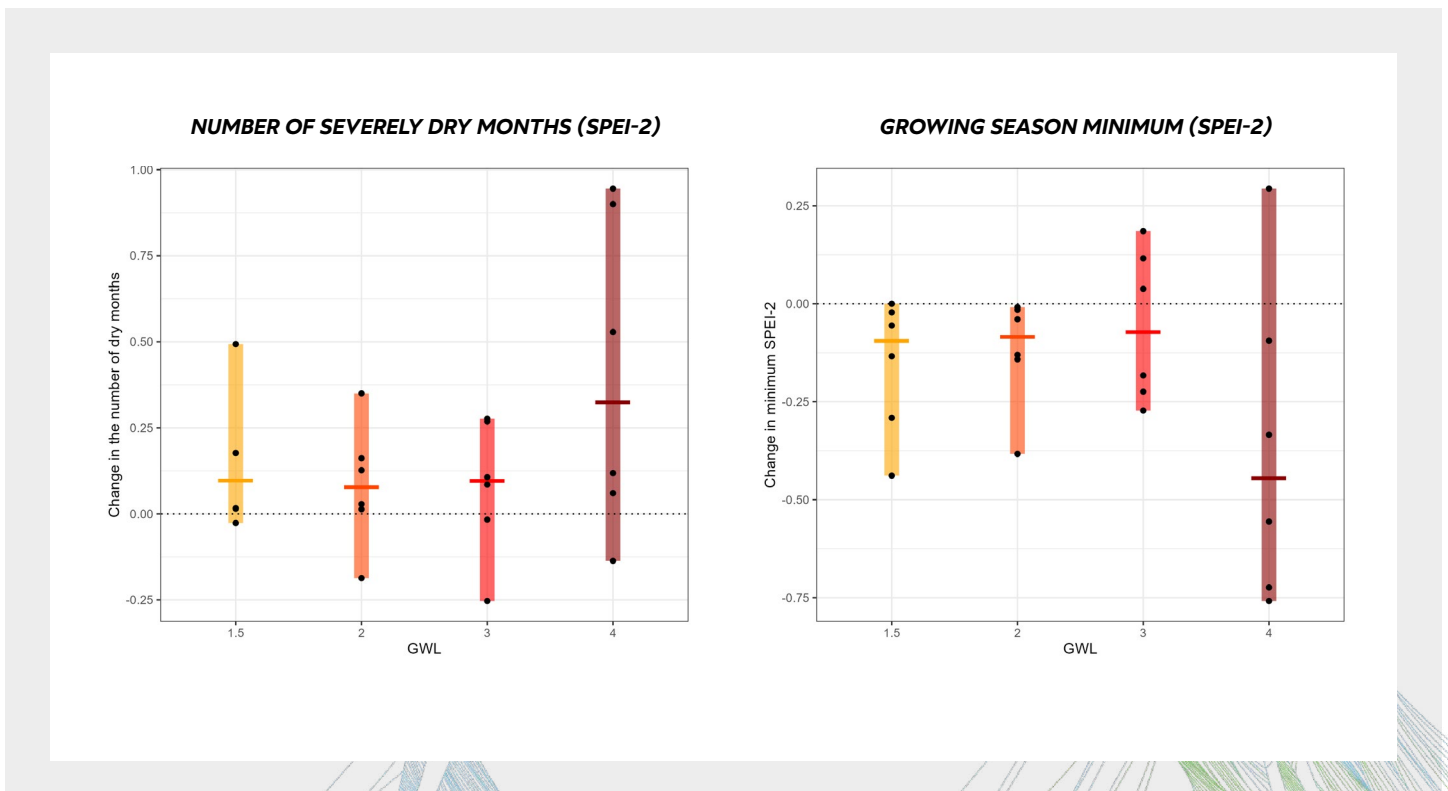


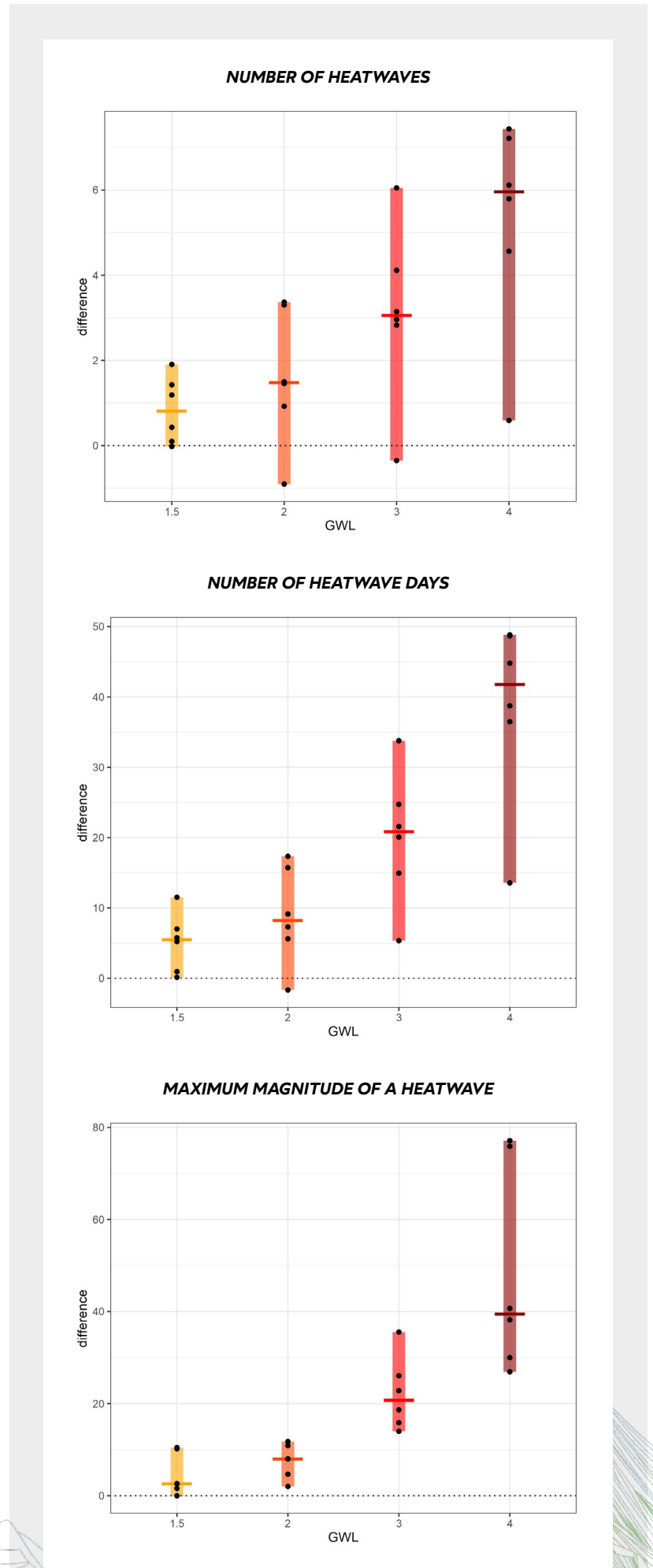
**FIGURE 16:** Change in the number of at least severely dry months (SPEI-2) and in minimum SPEI-2 in growing season months for four global warming levels relative to 1991–2020, averaged over the Sora catchment area. The bars show the range and the median of the model ensemble.

## HOW WILL EXTREME HEATWAVES CHANGE?

In terms of heatwaves, heatwave days and the maximum magnitude of heatwaves, there is no doubt what the future holds (**FIGURE 17**). An increase of around 2 to 3 additional heatwaves per year compared to the reference period is anticipated, which corresponds to a 50 to 100 % increase. Heatwave days and the maximum magnitude of a heatwave will double. To illustrate, during the reference period (1991–2020), the most intense heatwave had a magnitude equal to 128. However, under scenarios where global warming reaches 3 °C or more, such an event would no longer rank among the most severe annual occurrences; instead, it would be considered as an average heatwave.

This is further supported by the increasing probability of occurrence of extreme heatwaves in the future. A heatwave event as extreme as the 1-in-50-year event in 1991–2020 is projected to become up to 8.3 times as likely under GWL 3 °C and 16.7 times as likely under GWL 4 °C. In other words, a 50-year event in the reference period might become a 6-year event in a 3 °C warmer climate and a 3-year event in a 4 °C warmer climate.

**FIGURE 17:** Change in the number of heatwaves, the number of heatwave days and the maximum magnitude of a heatwave in a year for four global warming levels relative to 1991–2020, averaged over the Sora catchment area. The bars show the range and the median of the model ensemble.



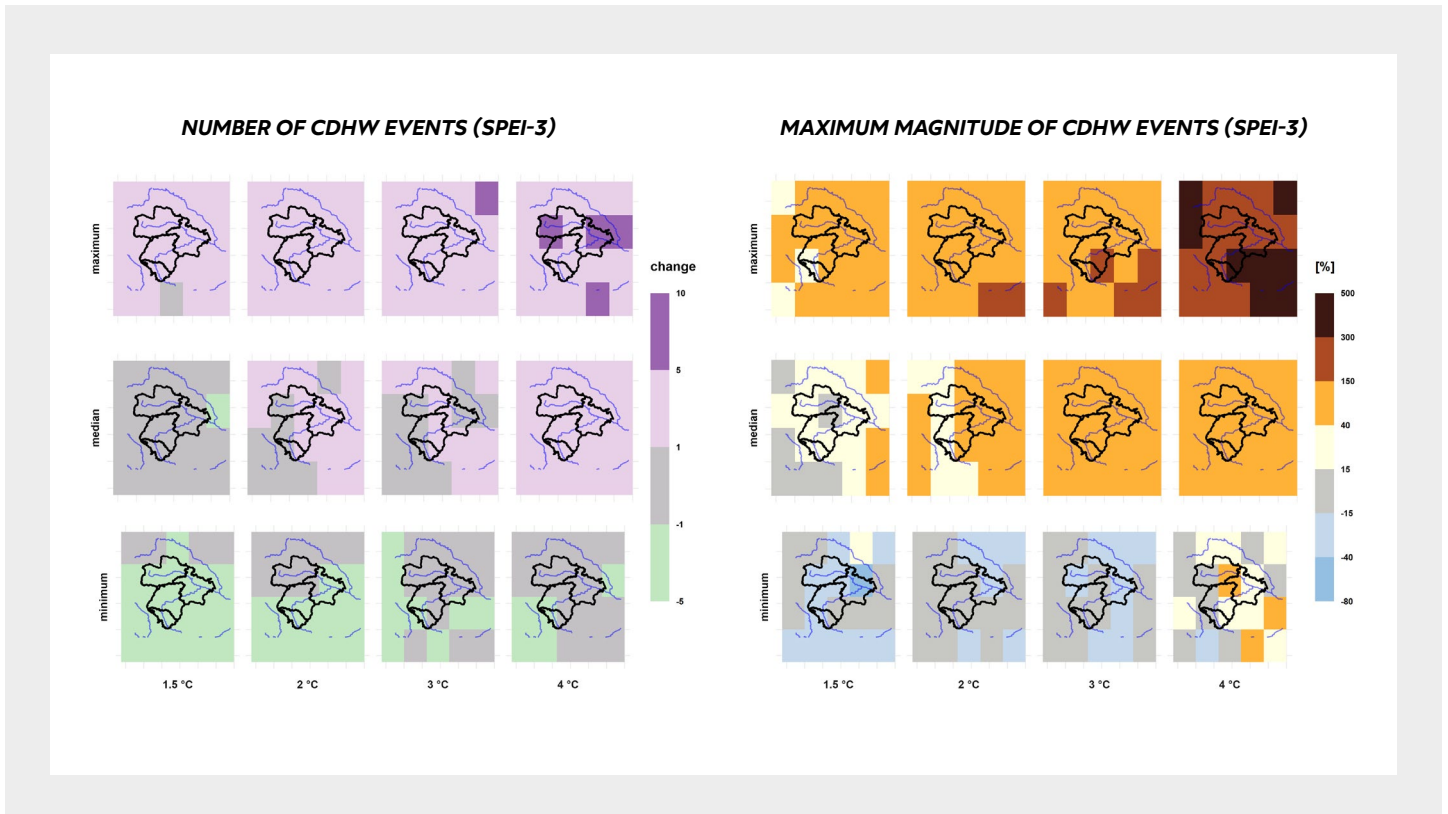


**FIGURE 18:** Change in the number and maximum annual magnitude of compound drought and heatwave events for four global warming levels relative to 1991–2020. The top, middle and bottom row show the maximum, median and minimum of the model simulation ensemble, respectively.

## HOW WILL COMPOUND DROUGHT AND HEATWAVE EVENTS CHANGE?

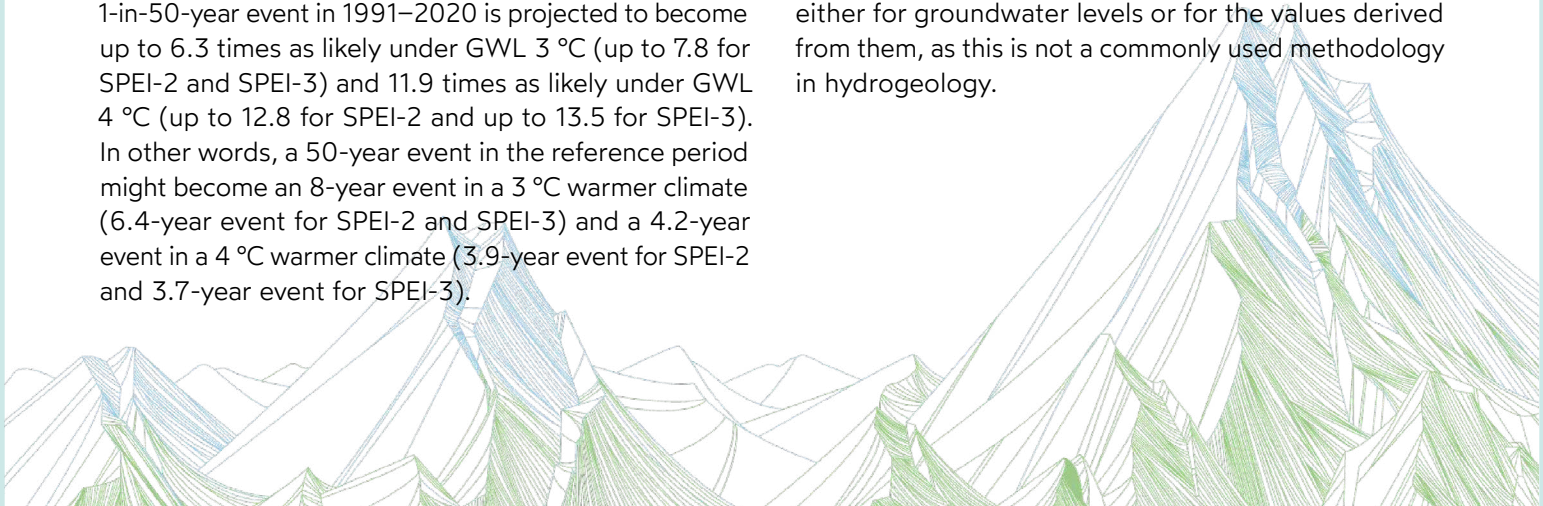
The frequency of compound drought and heatwave events is expected to increase by 1 to 5 events per year under GWL 3 °C and GWL 4 °C (**FIGURE 18** left), corresponding to a relative increase from 15 to over 100 %. Regardless of the specific global warming level anticipated, future events are expected to intensify (**FIGURE 18** right). The median estimate across models suggests intensification of compound events ranging from 40 % to 150 %.

Similarly as for individual drought and heatwave events, the occurrence of extreme drought and heatwave events is also expected to increase in the future. A compound drought (SPEI-1) and heatwave event as extreme as the 1-in-50-year event in 1991–2020 is projected to become up to 6.3 times as likely under GWL 3 °C (up to 7.8 for SPEI-2 and SPEI-3) and 11.9 times as likely under GWL 4 °C (up to 12.8 for SPEI-2 and up to 13.5 for SPEI-3). In other words, a 50-year event in the reference period might become an 8-year event in a 3 °C warmer climate (6.4-year event for SPEI-2 and SPEI-3) and a 4.2-year event in a 4 °C warmer climate (3.9-year event for SPEI-2 and 3.7-year event for SPEI-3).

## HOW WILL GROUNDWATER DROUGHT CHANGE?

In the future, net groundwater recharge (Q<sub>rn</sub>) in the period from March to August is expected to remain similar to the median values in the reference period 1991–2020, mainly due to winter and spring precipitation (**FIGURE 19**). The greatest increase in net groundwater recharge is expected to occur at the control point Praprotno II (by around 10 % under GWL 4 °C), however, due to the large spread, it is not possible to speak of a reliable change.

The SGI values at all measuring points in Slovenia have not yet been evaluated based on climate scenarios until the end of the 21<sup>st</sup> century. For now, we can only rely on existing data. Return periods have not been calculated either for groundwater levels or for the values derived from them, as this is not a commonly used methodology in hydrogeology.



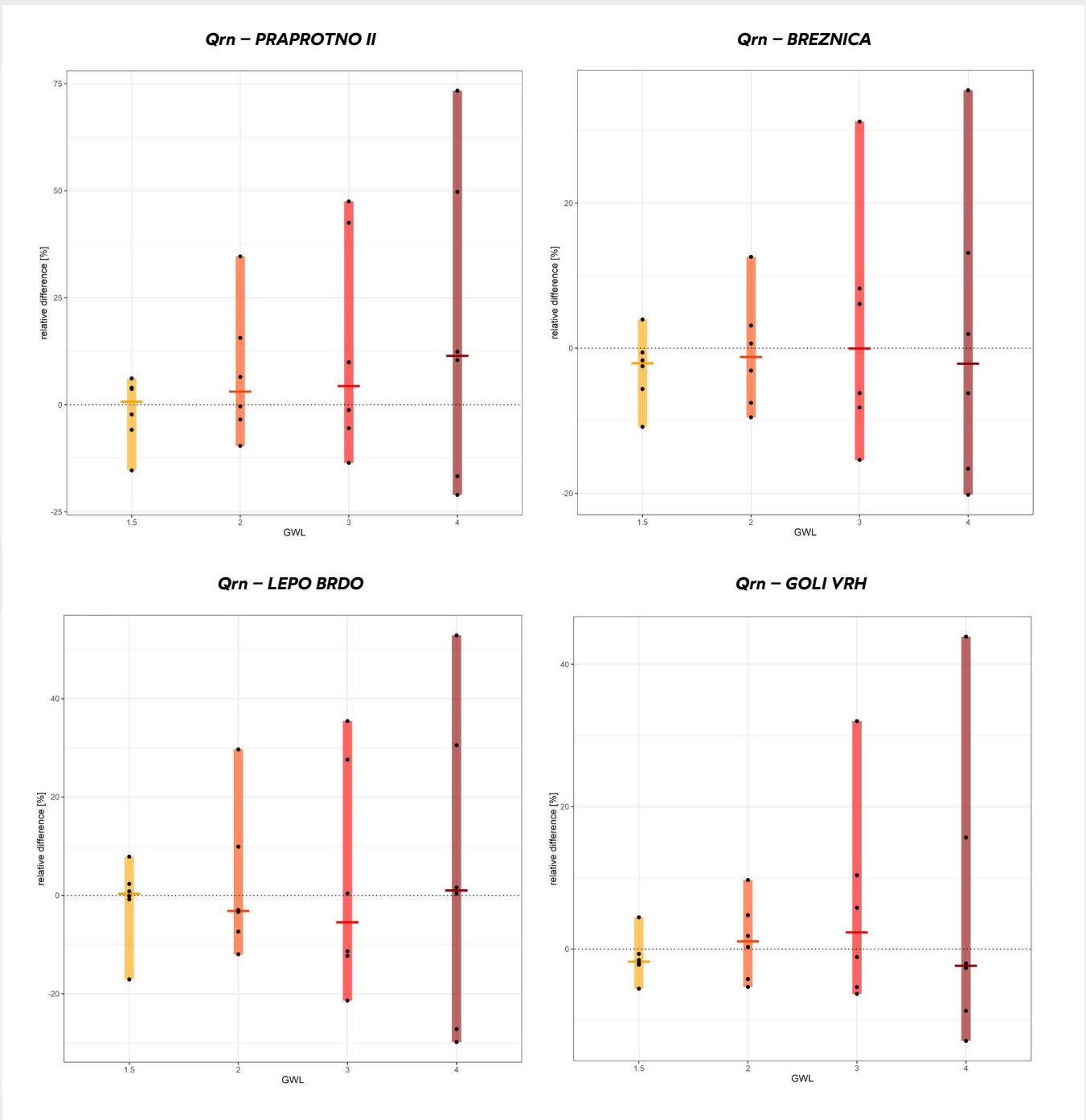


**FIGURE 19:** Change in the *Qrn* values at the four control points in the period from March to August for four global warming levels relative to 1991–2020. The bars show the range and the median of the model ensemble.



# METHODOLOGY



## ASSESSMENT OF TRENDS AND PROBABILITY OF OCCURRENCE

Trends, except trends in extreme values, were assessed with Theil-Sen estimator. The frequency of extreme values was estimated with classical extreme value theory (fitting corresponding data to the generalised extreme value distribution), and trends in extreme values with non-stationary extreme value theory. The methodology of each method is briefly described below.

### Trend assessment with Theil-Sen estimator

Trends for values not connected to extreme values were estimated with Theil-Sen estimator or Sen's slope estimator. This is a robust method of linear regression that is not influenced by outliers. It is nonparametric method and does not assume any specific distribution for the data. On the other hand, it is hardly less reliable in the cases where all conditions for the least square method are met. Calculation of trends is quite simple: it is the median of all possible slopes formed by pairs of points for a given collection of data points. Each pair contributes to the slope calculation, regardless of whether the points lie on a straight line or not. At the same time an accurate confidence interval for the trend can be estimated even when there are nonnormality and heteroscedasticity (Wilcks, 2016).

Statistical significance of the time series was assessed with Mann-Kendall trend test. It is a nonparametric test, without assuming normality, but the data should have no serial correlation. The null hypothesis was rejected when the p-value associated with Mann-Kendall statistics was lower than 0.05 or 0.10 respectively. Non-serial correlation, if existed, was achieved by Zhang's method of pre-whitening (Wang and Swail, 2001).

### Generalized extreme value distribution (GEV) and estimation of return periods of extreme events

The probability of extreme events was calculated with classical extreme value theory. The classical extreme value theory focuses on the statistical behaviour of extreme values of block maxima, usually corresponding to the annual or seasonal maxima. If the process is stationary, then under quite common conditions, for some large value of blocks (which in our case corresponds to the number of years) block maxima have a limiting distribution, called *generalised extreme value distribution* (GEV distribution) (Coles, 2001). The GEV distribution is a family of continuous probability distributions with three parameters: location ( $\mu$ ), scale ( $\sigma$ ) and shape parameter ( $\xi$ ).

Block maxima are fit to GEV distribution with maximum likelihood estimation, which also makes possible the estimation of confidence intervals for parameters and return levels.

Estimates of extreme quantiles of the annual maximum distribution were obtained from the GEV distribution and expressed in the form of return levels  $z_p$ . The return level  $z_p$  is associated with the return period  $1/p$ , where  $p$  is the probability of occurrence for the value  $z_p$  or more. More precisely,  $z_p$  is exceeded by the annual maximum in any particular year with probability  $p$  (Coles, 2001).

If a large number of years considered had study quantity equal to zero, the probability for the selected event was adjusted. This adjustment was made by dividing the probability by the ratio of years with non-zero data and total number of years for which data were available.





## Trend assessment for extreme values

The GEV distribution is valid for block extremes for stationary sequence. It can be generalised to non-stationary processes, e.g. for those with trends, possibly due to long-term climate changes. This can be achieved with GEV distribution with time dependent parameters; in our case appropriate model was linear in location parameter only:

$$\mu(t) = \mu_0 + \mu_1 t$$

The parameter  $\mu_1$  corresponds to the annual rate of change in annual maximum value of the variable it concerns. For linear model that means that the levels with all return periods change for the same amount in time. More complex models were also examined but they were mostly statistically insignificant. Statistical significance of the models is checked with the *likelihood ratio test* (Coles, 2001).

## ANALYSIS OF PROJECTED CHANGES UNDER DIFFERENT GLOBAL WARMING LEVELS

The projected changes in the pilot area were assessed for different levels of global warming by considering the available EURO-CORDEX projections listed under Data. The global warming levels (GWLs) considered were + 1.5, + 2, + 3 and + 4 °C with respect to the pre-industrial baseline period 1850-1900, following the approach included in the Sixth Assessment Report of the Intergovernmental Panel on Climate Change (IPCC, 2021). For each GWL, the corresponding 20-year period when global mean temperature reaches that level of increase with respect to the baseline period was identified for each model and RCP (Representative Concentration Pathway) simulation

([https://github.com/mathause/cmip\\_warming\\_levels](https://github.com/mathause/cmip_warming_levels)). Since some models and RCP scenarios do not include all GWLs, only simulations covering all considered GWLs were considered, namely RCP 8.5 simulations.

It is important to note, that GWLs cannot be translated into a specific temporal interval since it varies among the models. However, for assigning a temporal horizon to projected results, the highest GWL 3 °C and GWL 4 °C are reached by models in the second half of the 21<sup>st</sup> century under high emission scenarios.

For the assessment of future changes and return periods, the 20-year interval associated with each GWL was considered and extended over a 30-year period by adding 5 years before and after the GWL interval. Projected changes were evaluated for selected model simulations relative to the 1991–2020 baseline and reported as model ensemble median and range.

## ANALYSIS OF SYNOPTIC CONDITIONS FOR PILOT EVENTS

Mean sea level pressure (MSLP) data from -80° West to 40° East and 30° to 70° North for the last 70 years from the ERA5 reanalysis was used to calculate 'Gross-Wetter-Typen' (GWT), which is a circulation type classification and is based on correlations between mean sea level pressure fields that are grouped into 18 clusters. The COST733 (Philip et al., 2014) software was used for that. Specific pilot events were then characterised by the mean GWT pattern derived over 7 decades of ERA5 data and by analysing the specific daily MSLP pattern at event occurrence. Furthermore, for the specific season when the event has happened, trends in GWT occurrences over the 70-year period were evaluated with a 99 % confidence interval.



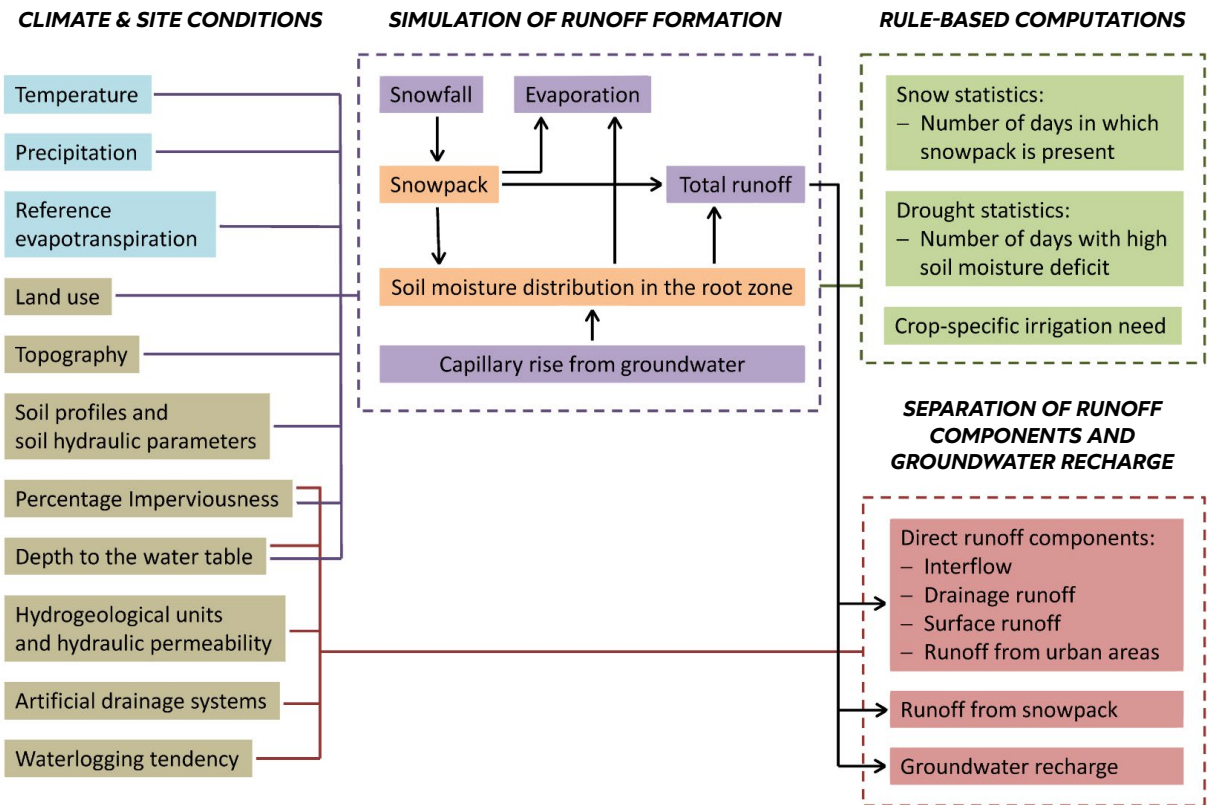


FIGURE 20: mGROWA modelling concept (Source: Frantar, Tetzlaff, Wendland, Andjelov, 2018)

## ANALYSIS OF GROUNDWATER DROUGHT WITH mGROWA

mGROWA – monthly *GROßräumiges Wasserhaushaltsmodell* (Regional Water Balance Model) developed at Forschungszentrum Jülich, is a grid based empirical regional model consisting of several modules, enabling separation of input precipitation into main water balance components: real evapotranspiration, total discharge, direct runoff and groundwater recharge. It calculates net water balance, originating only from precipitation at modelled area. Model mGROWA is an upgrade of previous model GROWA which has yearly temporal resolution (Frantar, Tetzlaff, Wendland, Andjelov, 2018).

Simplified hydrological processes are modelled in 100 m raster cells. The geographic inputs to the model are land use, topography, impervious surfaces, soils and features, depth to water table, hydrogeological units and permeability, drainage, waterlogging tendency. The

hydrological model is based on meteorological input data: precipitation and potential evaporation, as well as meteorological data for snow cover simulation (Frantar, Herrmann, Andjelov, Draksler, Wendland, 2018).

Runoff is one of the main outputs of the model. The total runoff is split up into components, the primary ones being groundwater recharge and direct runoff. A very useful product in drought analyses is also the SWD indicator - an indicator of soil water deficit. The model method is set to daily or monthly time scale, which makes it possible to perform seasonal analyses of water balance components for all of Slovenia.

In addition to reference calculations, the mGROWA model also enables scenario-based analyses of climate change. On the basis of the input data of the climate scenarios, we can calculate all the results of the water balance elements in a changed climate (Frantar, Herrmann, Andjelov, Draksler, Wendland, 2018).

# REFERENCES



- Andjelov, M., Mikulič, Z., Tetzlaff, B., Uhan, J., Wendland, F., 2016. Groundwater recharge in Slovenia: Results of a bilateral German-Slovenian research project. *Energy & Environment*, Jülich, 145 pp.
- Bertalaníč et al., 2018. Ocena podnebnih sprememb v Sloveniji do konca 21. stoletja: sintezno poročilo. Ministrstvo za okolje in prostor, Agencija Republike Slovenije za okolje, Ljubljana.
- Coles, S., 2001. *An Introduction to Statistical Modeling of Extreme Values*. Springer, London, 209 pp.
- Copernicus C3S, 2023. *European State of the Climate 2022 Summary*. URL: <https://climate.copernicus.eu/esotc/2022/european-state-climate-2022-summary>
- Frantar, P., Herrmann, F., Andjelov, M., Draksler, A., Wendland, F., 2018. Vodnobilančni model mGROWA-SI. 29. *Mišičev vodarski dan – Zbornik referatov*. 6<sup>th</sup> December 2018, Maribor. URL: <https://www.mvd20.com/LETO2018/R27.pdf>
- Frantar, P., Tetzlaff, B., Wendland, F., Andjelov, M., 2018. Regional Water Balance Modelling by mGROWA in Slovenia.
- Herrmann, F., Keller, L., Kunkel, R., Vereecken, H., Wendland, F., 2015. Determination of spatially differentiated water balance components including groundwater recharge on the Federal State level – A case study using the mGROWA model in North Rhine-Westphalia (Germany). *Journal of Hydrology: Regional Studies*. 294-312, doi: [10.1016/j.ejrh.2015.06.018](https://doi.org/10.1016/j.ejrh.2015.06.018)
- IPCC, 2021. *Climate Change 2021: The Physical Science Basis. Contribution of Working Group I to the Sixth Assessment Report of the Intergovernmental Panel on Climate Change* [Masson-Delmotte, V., P. Zhai, A. Pirani, S.L. Connors, C. Péan, S. Berger, N. Caud, Y. Chen, L. Goldfarb, M.I. Gomis, M. Huang, K. Leitzell, E. Lonnoy, J.B.R. Matthews, T.K. Maycock, T. Waterfield, O. Yelekçi, R. Yu, and B. Zhou (eds.)]. Cambridge University Press, Cambridge, United Kingdom and New York, NY, USA, In press, doi: [10.1017/9781009157896](https://doi.org/10.1017/9781009157896)
- Pavlič, U., 2024. Hidrološka suša podzemnih vod. Kazalci ARSO. URL: <https://kazalci.arso.gov.si/sl/content/hidroloska-susa-podzemnih-voda-0>
- Philipp, A., Beck, C., Esteban, P., Kreienkamp, F., Krennert, T., Lykoudis, S.P., Pianko-Kluczynska, K., Post, P., Rasilla-Alvarez, D., Spekat, A., Streicher, F., 2014. *COST733CLASS v1.2 User guide*.
- Scherrer, S. C., Fischer, E. M., Posselt, R., Liniger, M. A., Croci-Maspoli, M., Knutti, R., 2016. Emerging trends in heavy precipitation and hot temperature extremes in Switzerland. *J. Geophys. Res. Atmos.*, 121, 2626-2637, doi: [10.1002/2015JD024634](https://doi.org/10.1002/2015JD024634)
- Strgar, A., Frantar, P., 2018. Kazalnik suše SWD vodnobilančnega modela mGROWA-SI za Slovenijo. *Ujma*, 33, 104-111. URL: [https://www.gov.si/assets/organi-v-sestavi/URSZR/Publikacija/Ujma/2019/104-111\\_vsebina\\_za\\_tisk.pdf](https://www.gov.si/assets/organi-v-sestavi/URSZR/Publikacija/Ujma/2019/104-111_vsebina_za_tisk.pdf)
- Wang, X. L., and Swail, V. R., 2001. Changes of Extreme Wave Heights in Northern Hemisphere Oceans and Related Atmospheric Circulation Regimes. *J. Climate*, 14, 2204-2221, doi: [10.1175/1520-0442\(2001\)014<2204:COEWHI>2.0.CO;2](https://doi.org/10.1175/1520-0442(2001)014<2204:COEWHI>2.0.CO;2)
- Wilcox, R. R., 2001. *Fundamentals of Modern Statistical Methods*. Springer, New York, 258 pp.
- Zhang, Q., She, D., Zhang, L., Wang, G., Chen, J., Hao, Z., 2022. High sensitivity of compound drought and heatwave events to global warming in the future. *Earth's Future*, 10, doi: [10.1029/2022EF002833](https://doi.org/10.1029/2022EF002833)

